High Resolution Laser Spectroscopy

By G. Duxbury
DEPARTMENT OF PHYSICS, THE UNIVERSITY OF STRATHCLYDE,
107 ROTTENROW, GLASGOW G4 0NG

1 Introduction

The rapid development of lasers since their first use as molecular spectroscopic tools in 1964, has resulted in very high resolution spectrometers becoming available for the wavelength region from the infrared to the ultraviolet, *i.e.* from 1 mm to 300 nm. The availability of laser sources has completely transformed atomic and molecular spectroscopy by providing a *sensitivity*, *resolution*, and *selectivity* several orders of magnitude greater than previously available. The development of laser based systems parallels that of the earlier NMR and ESR spectrometers. The first decade after the discovery of the physical principles of the devices was primarily the province of physicists, who developed the techniques and the theoretical understanding of the processes involved in the interaction of coherent radiation with atomic and molecular systems, whereas in the second decade chemists have been applying these new radiation sources to systematic molecular spectroscopy. The parallel between laser spectrometers and magnetic resonance systems extends to a comparison of particular experiments, since many of the laser-based experiments are the optical analogues of those previously developed in the microwave and the radiofrequency regions.

One area of particular interest in laser spectroscopy has been the study of free radicals such as NH_2 and CH_3, in order to obtain a detailed knowledge of their potential energy surfaces in different electronic states. Other topics that have been treated in some detail are the experimental investigation of the variation of molecular dipole moments with electronic, vibrational, and rotational state, and the monitoring of state selective processes, where the definition of a 'state' includes the possibility of velocity group monitoring, which is precluded in the low frequency spectroscopic region of most microwave spectrometers, ten to forty GHz.

In this article we will consider both the armoury of techniques now available for carrying out high resolution spectroscopy and also the use of combinations of the methods for studying small polyatomic molecules, which are of considerable interest because of their role in chemical reactions, or in testing current models of vibration–rotation interaction and of dipole moment variation.

2 Principles of Sub-Doppler Spectroscopy

In order to appreciate the reasons for the high resolution and the high sensitivity of laser spectroscopy it is first of all necessary to consider the details of the

interaction between monochromatic high-power coherent sources and molecular absorbers. This comprises both the mechanisms of spectral line broadening in low pressure gases, and the perturbations of the line shape associated with the strong laser radiation field. The various types of available spectrometers can then be classified not only from the point of view of the resolution and the selectivity available, but also from the standpoint of analogies between laser spectrometers and magnetic resonance or microwave spectrometers currently in use in university chemistry departments.

A. Line Broadening in Low-pressure Gases, Homogeneous, and Inhomogeneous Line Shapes.—Line broadening mechanisms in low-pressure gases can be classified into two types, homogeneous and heterogeneous. A similar classification was originally developed for line shapes in magnetic resonance spectroscopy.[1,2] Homogeneous processes are associated with the uncertainty principle, some decay process prevents the molecule remaining in a specified energy state for longer than a time interval Δt on average, and the line width $\gamma = 1/\Delta t$. The principal contributions to this linewidth in gases are collisional broadening, when γ is proportional to pressure; power or saturation broadening, which depends upon the rate at which the molecules are transferred between the upper and the lower energy states by the radiation field; and radiative decay of the excited-state level leading to natural line broadening. The natural contribution to the linewidth is particularly important when electronically excited states are involved in a transition. In laser spectroscopy a further mechanism becomes operative, transit-time broadening, which is caused by the molecules spending only a finite time in the radiation field as they pass through the laser beam.

The general form of a homogeneously broadened line is Lorentzian, with the absorption coefficient given by

$$\alpha(\nu) = \frac{S_1}{\pi} \frac{\gamma}{(\nu - \nu_0)^2 + \Gamma^2} \tag{1}$$

where Γ, the power broadened line width is given by:

$$\Gamma^2 = (\gamma^2 + |\mu_{12}|^2 E^2/h^2) \tag{2}$$

and γ, the half width at half height in the absence of saturation, is the sum of contributions from natural linewidth, pressure broadening, and transit time effects. $|\mu_{12}|$ is the transition dipole matrix element between levels 1 and 2, which we will abbreviate as μ, E is the electric field amplitude of the incident radiation field, and S_1 is the integrated absorption coefficient for the line.

Heterogeneous line broadening in gases is associated with the Doppler effect. If a moving molecule emits radiation, the emitted frequency is not centred at the resonant frequency of the molecular transition, but is shifted by an amount which

[1] J. I. Steinfeld, 'Molecules and Radiation: An Introduction To Modern Molecular Spectroscopy', Harper and Row, 1974.
[2] W. Demtroder, 'Laser Spectroscopy', Springer Verlag, 1981.

depends on the component of the molecular velocity in the direction of the emitted radiation. The Doppler effect occurs because the moving wave fronts of the emitted radiation are compressed in the direction of the molecule's motion, and are expanded in the opposite direction, giving rise to a shift in wavelength and hence in frequency. The apparent emission frequency is increased if the molecule moves towards the observer, and is decreased if the molecule moves away. A similar effect occurs if we consider the absorption of radiation by a molecule. If we choose the $+z$ direction in the laboratory to coincide with the direction of propagation of a laser beam, the frequency ν_1 of a laser in the laboratory frame of reference appears in the frame of reference moving with the molecule as:

$$\nu' = \nu_1(1 - v_z/c) \tag{3}$$

where v_z is the component of the molecular velocity along the z direction in the laboratory frame. The molecule can only absorb radiation if ν' coincides with its absorption frequency ν_0, *i.e.* $\nu_1 = \nu_0(1 + v_z/c)$. The absorption frequency of the laser radiation is thus higher than the centre frequency if v_z is positive, *i.e.* if the molecule moves parallel to the wave propagation direction, and is lower than the centre frequency if v_z is negative, *i.e.* the molecule moves in the opposite sense to the direction in which the laser beam is propagating. These effects are shown schematically in Figure 1.

The components of the molecular velocities along a fixed direction in a gas at thermal equilibrium at a temperature T obey the Maxwell distribution,

$$w(v_z) = (1/u\sqrt{\pi})\exp(-v_z^2/u^2) \tag{4}$$

where $u^2 = 2kT/m$, m is the molecular weight and k is Boltzmann's constant. This gives rise to the Gaussian lineshape

$$\alpha(\nu) = \frac{S_1}{\delta\sqrt{\pi}}\exp -\left[\frac{\nu - \nu_0}{\delta}\right]^2 = \alpha_0 \exp -\left[\frac{\nu - \nu_0}{\delta}\right]^2 \tag{5}$$

where the half width parameter δ is given by

$$\delta = \nu/c\sqrt{\frac{2kT}{m}}$$

The half width at half height is related to δ by $\delta(\ln 2)^{\frac{1}{2}}$, and that at maximum slope by $\delta/\sqrt{2}$.

Line shapes in gases are governed by both the homogeneous and the heterogeneous contributions. In the infrared region the line shape may be considered to be made up from a large number of Lorentzian curves, one for each group of molecular velocities. This is shown schematically in Figure 1. The resultant line shape is a convolution of the Gaussian and the Lorentzian contributions, and is known as the Voigt line shape. In the spectra of many molecules observed at wavelengths shorter than 20 μm, the predominant source of line broadening is the Doppler effect, with the homogeneous contribution to the overall linewidth being at least a factor of one hundred times smaller than the heterogeneous Doppler contribution. The partial or almost complete elimination

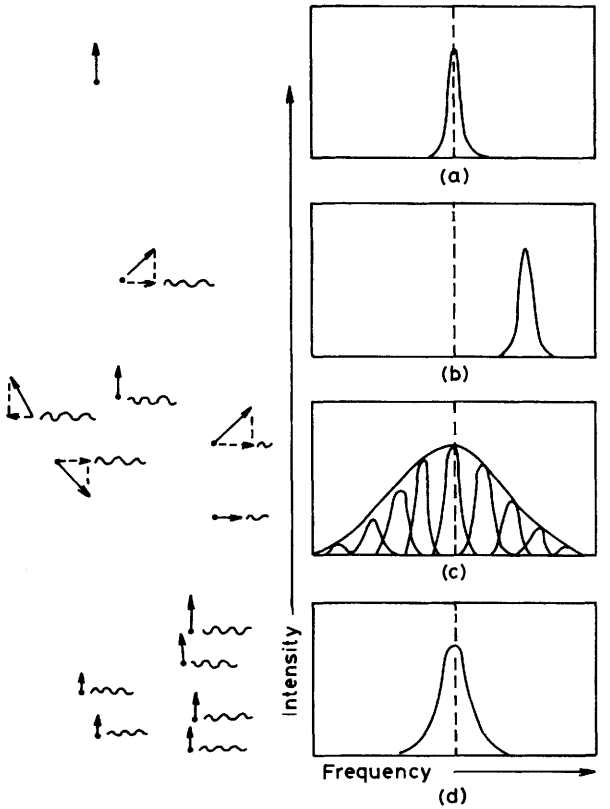

Figure 1 *Influence of the Doppler effect on the width of a spectral line. (a) Homogeneous (Lorentzian) line shape, centred at ν_0, if particle is moving perpendicular to the laser beam direction, z. (b) Doppler-shifted line position for one velocity component along z. (c) Envelope of the line shapes of (a) and (b) produced when particles can move in all directions. (d) In a molecular beam, the spread of velocities along the z direction is small; area (a) is almost recovered*

of the Doppler contribution to line broadening thus results in a very great enhancement of the resolution.

The oldest form of sub-Doppler spectroscopy is atomic or molecular beam spectroscopy, in which a collimated beam of atoms or molecules is directed at right angles to the radiation field. The reduction in Doppler broadening obtainable is then dependent upon the spread of the beam. The main problems encountered are associated with the low pressures in molecular beam spectrometers, which limits the sensitivity of the system, and with the difficulties inherent in producing intense, well collimated beams. The more recent methods of sub-Doppler spectroscopy make use of the properties *of the radiation field itself* to pick out a particular velocity group from the random set of molecules in the bulk gas sample in the cell.

This results in a higher sensitivity than is generally achievable in molecular beam experiments, it also results in much higher resolution than can usually be obtained using molecular beam spectrometers in the infrared and the visible spectral regions.

B. Saturation Effects and Sub-Doppler Linewidths.—If we now consider the effect of a strong saturating field produced by a laser on a predominantly heterogeneously broadened molecular absorption line, we can see from the discussion in Section A that the effect will be confined to a narrow region centred upon the velocity component of the group of molecules whose absorption is Doppler shifted into resonance. This produces a 'hole' in the population of the lower state and a 'spike' in the population of the upper state, resulting in a 'hole' in the absorption profile. This 'hole burning' model is due to Bennett[3] and is shown schematically in Figure 2 for interaction of molecules with a running wave propagating in the $+z$ direction. Since the molecular velocity component at resonance will have a homogeneously broadened lineshape, the 'hole', which depends upon the partial saturation of the Lorentzian line centred at v_z, will also have a Lorentzian shape. Thus the 'hole' can frequently be treated as an absorption feature with a negative absorption coefficient. The width of the hole is determined by the factors governing homogeneous line broadening, *i.e.*

$$\gamma_{\text{hole}} = \left[\gamma^2 + \left(\frac{\mu E}{h}\right)^2\right]^{\frac{1}{2}} = \Gamma \tag{6}$$

The various methods of saturation spectroscopy rely on detecting this narrow hole by differential saturation effects, and hence achieving considerable resolution enhancement. Hole burning is really a description of the effect of the strong fields on the energy level populations and can be described quantitatively using a rate equation model, but it omits coherent excitation processes, which are sometimes very important.

Some of the principal schemes for experiments based on velocity selection using the properties of the laser radiation field are sketched in the remainder of this section.

C. Lamb Dips.—If the molecules are subjected to a standing wave field, holes are burned on both sides of the centre frequency as shown in Figure 2. At line centre the holes coalesce, corresponding to one group of molecules with zero velocity component along the direction of the standing wave field interacting with both running waves' components. This double saturation interaction results in a sharp dip in the absorption coefficient at line centre. This effect was first seen as a dip in the gain of atomic gas lasers[4] and slightly later as a dip in the absorption of an intracavity sample, giving rise to an increase of laser power at the centre of the saturated absorption line. It is for this reason that the absorption feature was initially known as an inverted Lamb dip.[5] The change in the absorption coefficient

[3] W. R. Bennett, *Phys. Rev.*, 1962, **126**, 580; *Comments on Atomic and Molecular Physics*, 1970, **2**, 1.
[4] R. A. McFarlane, W. R. Bennett, and W. E. Lamb, *Appl. Phys. Lett.*, 1963, **2**, 189.
[5] P. H. Lee and M. C. Skolnick, *Appl. Phys. Lett.*, 1967, **10**, 303.

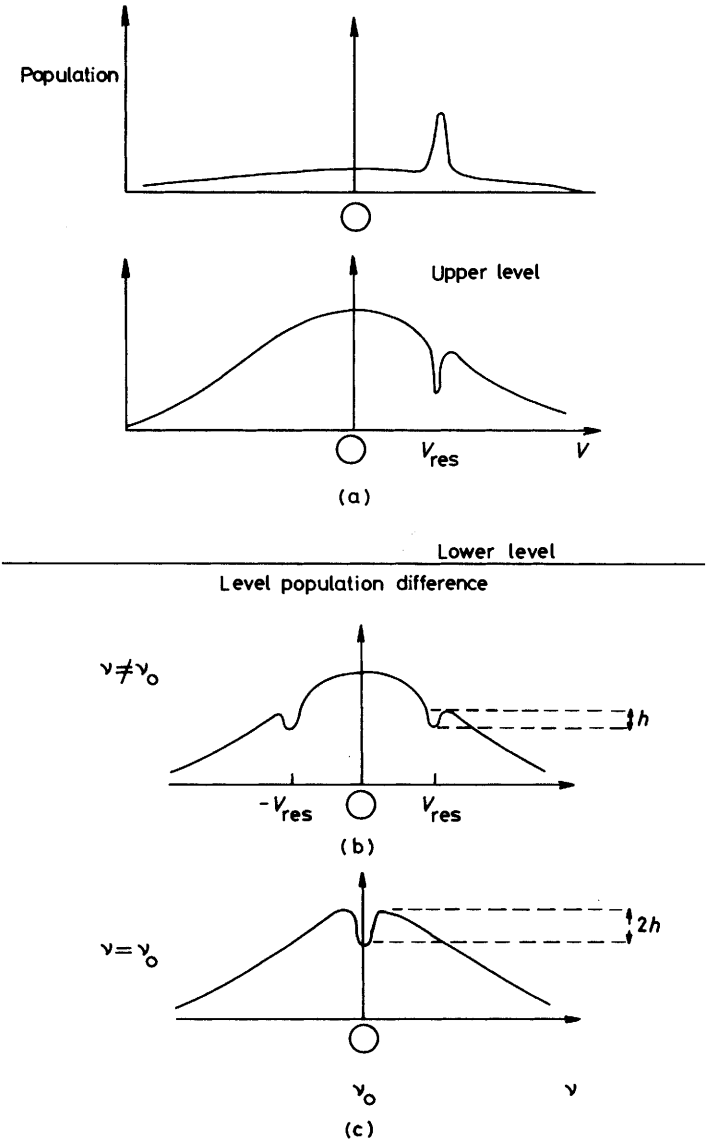

Figure 2 *Saturation of an inhomogeneously broadened line. (a) Changes in particle velocity distribution under the action of a laser of frequency* ν. *The z component of velocity of the particles interacting with the light wave is* $v_{res} = c\,(\nu - \nu_0)\,/\nu_0$. *A Bennett hole is generated in the lower level and a population peak in the upper level. (b) Changes in population difference induced by a standing wave of resonance,* $\nu \neq \nu_0$. *(c) On resonance,* $\nu = \nu_0$, *a double saturation effect is observed at line centre, the* Lamb dip

between that which is observed using a standing wave field, and that which would be observed using a running wave over the same path length, can be denoted as the 'effective absorption coefficient' of the Lamb dip. This is given by $\Delta\alpha(\nu) = \alpha(\nu)_{\text{standing}} - \alpha(\nu)_{\text{running}}$:

$$\Delta\alpha(\nu) = -2\alpha_0 A \frac{(\Gamma + \Gamma')^2}{(2\nu - 2\nu_0)^2 + (\Gamma + \Gamma')^2} \tag{7}$$

Where Γ and Γ' are the power saturated half-widths of the 'hole' for the forward and the backward running wave fields, and A is a 'saturation parameter' dependent on the level of saturation of the absorption line.

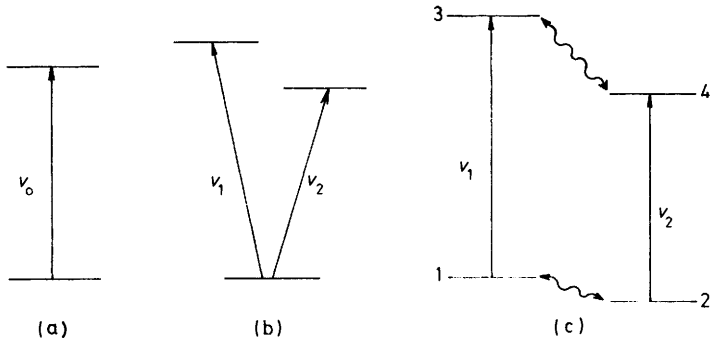

Figure 3 *Schematic energy level diagrams illustrating (a) single resonance, (b) three-level double resonance and (c) four-level double resonance. The wavy arrows in (c) represent collision induced transitions*
(Reproduced by permission from *J. Chem. Phys.*, 1975, **62**, 1488)

D. Velocity-tuned Three- and Four-level Resonances.—When two transitions share a common level and their transition frequencies overlap to within about two Doppler widths of each other, three-level 'crossover' resonances can be seen in addition to the 'normal' Lamb dips.[6] A schematic energy level diagram is given in Figure 3. The effects of saturating one of the transitions can be probed *via* the second transition. The velocity matching condition for the velocity group, v_m, for which this occurs is given by

$$\Omega(1 + v_m/c) = \nu_1 \text{ and } \Omega(1 - v_m/c) = \nu_2 \quad \text{or}$$
$$\Omega(1 + v_m/c) = \nu_2 \text{ and } \Omega(1 - v_m/c) = \nu_1 \tag{8}$$

That is the oscillating fields E_+ and E_- of the laser, frequency Ω, affect molecules with the same velocity v_m by means of different transitions, ν_1 and ν_2. This causes centre dips at the frequency $\Omega = (\nu_1 + \nu_2)/2$, and

$$v_m = \pm c\frac{(\nu_1 - \nu_2)}{2\Omega} \neq 0$$

[6] H. R. Schlossberg and A. Javan, *Phys. Rev.*, 1966, **150**, 267.

The intensity of the 'centre dip' is related to that of the adjacent Lamb dips, and to the degree of Doppler mismatch by

$$\Delta\alpha(\nu) = (\Delta\alpha_1\Delta\alpha_2)^{\frac{1}{2}} \exp -\left[\frac{\Delta\nu}{2\delta}\right]^2 \tag{9}$$

where $\Delta\alpha_1$ and $\Delta\alpha_2$ are the intensities of the Lamb dips, and $\Delta\nu = \nu_1 - \nu_2$.

If pairs of two-level systems are coupled by collisional population transfer, where the collisions involve very little change in molecular velocities, four-level resonances may be observed, as first described by Shoemaker *et al.*[7] and by Johns *et al.*[8] This situation is shown schematically in Figure 3. The frequency-matching condition is identical to that for three-level resonances, but the intensities are different, since not all collisions are effective in coupling the levels within the four-level system without change in velocity, and may couple to other energy levels in the system, the heat bath. If we denote the rate of dip transferring transitions by k_Φ and the rate of transitions connecting the four-level system to the heat bath as k_ξ, the intensity of the four-level resonance is given by

$$\Delta\alpha(\nu) = (\Delta\alpha_1\Delta\alpha_2)^{\frac{1}{2}} \frac{2k_\Phi}{k_\Phi + k_\xi} \exp -\left[\frac{\Delta\nu}{2\delta}\right]^2 \tag{10}$$

The forces responsible for this effect are long range dipole–dipole interactions. The effects have mainly been observed as M_J changing collisions in Stark spectroscopy, and have been described as angular momentum tipping, or re-orientation, collision. The range over which they must occur has been estimated as *ca.* 20 Å.[8]

E. Optical–Optical Double Resonance and Level Crossing.—If a pair of transitions sharing a common level and overlapping to within about two Doppler widths interact with two co-propagating laser beams of different frequencies, a non-linear response will occur for the resonance condition[9, 2]

$$\Omega_1 - \Omega_2 = \nu_1 - \nu_2 \text{ or } \Omega_1 - \nu_1 = \Omega_2 - \nu_2 = \frac{v_z\bar{\nu}}{c} \tag{11}$$

where $\Omega_1 - \Omega_2$ is the difference frequency between the lasers, $\nu_1 - \nu_2$ is the difference frequency between the molecular transitions, and $\bar{\nu} \sim (\nu_1 - \nu_2)/2$. The energy level patterns for which this will occur are the 'vee' scheme of Figure 3, or its inverse the inverted 'vee'.

These experiments are usually carried out by keeping $\Omega_1 - \Omega_2$ fixed, and by varying $\nu_1 - \nu_2$ by the application of either an electric or magnetic field. Since the signal depends on a particular velocity group, v_z, being saturated, the linewidths are similar to those observed for Lamb dips.

If two or more overlapping transitions sharing a common level become accidentally degenerate at some value of an applied electric or magnetic field, a

[7] R. L. Shoemaker, S. Stenholm, and R. G. Brewer, *Phys. Rev. A*, 1974, **10**, 2037.
[8] J. W. C. Johns, A. R. W. McKellar, T. Oka, and M. Romheld, *J. Chem. Phys.*, 1975, **62**, 1488.
[9] R. G. Brewer, *Phys. Rev. Lett.*, 1970, **25**, 1639.

Doppler free non-linear signal can be seen at high laser power. In the two level case this is just the degenerate case of OODR, when two transitions become coupled at one laser frequency. This type of signal is most frequently seen at zero field when it is known as the zero field level crossing, or Hanle, signal. At zero field all the M_J components are degenerate, or crossed, and hence can all be saturated. Once a finite field is applied the M_J degeneracy is broken, and only some of the non-degenerate components of the transition can be saturated. Thus a differential saturation signal can be seen centred on zero field. This signal is seen in all cases in which OODR signals are observed, and helps to locate lines which are suitable for study. Since the position of the signal, whether at zero or at a finite field, depends only on the degeneracy of energy levels and not on the absolute transition frequency, its position remains invariant to laser drift. The zero field level crossing signal line shape is rather complicated because of the problems involved with the multiple degeneracy of the crossing levels.[10]

Linear level crossing signals were observed in pre-laser spectroscopy in the fluorescence excited by atomic lamps.[1] In the linear example a change in the angular dependence and the polarization characteristics of the emitted radiation occur, so that the fluorescence is monitored at right angles to the exciting beam. However, in the linear Hanle effect the *total* intensity radiated over all directions remains unchanged.

F. Anti-crossing.—If avoided crossings between Zeeman or Stark sub-levels occur, sub-Doppler spectra can be observed that resemble those obtained in level crossing experiments. When anti-crossing signals are observed in absorption it can be shown that the terms which account for the differential saturation detection of the avoided crossing are similar to those responsible for the observation of non-linear level crossing signals. Additional terms arise, however, from the variation of the transition dipole matrix elements from the common level to the two interacting levels. The matrix elements of the dipole moment operator have a very rapid variation in the crossing region, owing to the fact that at the point of nearest approach the wavefunctions of the two interacting states are almost a 50:50 mixture of the unperturbed functions. Anti-crossing signals have been observed both in laser Stark[11] and in laser magnetic resonance[12] experiments. The terms in the molecular Hamiltonian responsible for the production of the weak avoided crossings are usually higher-order terms that are neglected in the standard treatments of the Stark and Zeeman effects.

G. Doppler-free Two-photon Signals.—If we consider the interaction of a molecule with velocity v_z interacting with a standing wave field of frequency ν_1, in the frame of reference of the molecule the molecule interacts with two oppositely travelling

[10] M. S. Feld, A. Sanchez, A. Javan, and B. J. Feldman, in 'Methodes de Spectroscopie San Largeur Doppler de Niveaux Excites de Systemes Moleculaires Simples', CNRS No. 217 1974, p. 87.
[11] J. Sakai and M. Katayama, *Appl. Phys. Lett.*, 1976, **78**, 119.
[12] H. Uehara and K. Hakuta, *Chem. Phys. Lett.*, 1978, **58**, 287.

waves of frequencies $\nu_1(1 - v_z/c)$ and $\nu_1(1 + v_z/c)$ respectively. If the molecule can be excited from the ground to the excited state by the absorption of two photons, one from each of the oppositely directed travelling waves, then at resonance the following condition is fulfilled,

$$(E' - E'')/h = \nu_1(1 - v_z/c) + \nu_1(1 + v_z/c) = 2\nu_1 \qquad (12)$$

i.e. the resonance is independent of the velocity of the molecule, v_z.[2, 13, 14] In practice, two-photon transitions will be induced by the absorption of photons from travelling waves that are co-propagating, as well as the signal described above that results from the absorption of the two photons from counterpropagating waves. The Doppler-free two-photon signal will therefore be superimposed upon a broad Doppler broadened base, as shown in Figure 4. A fundamental difference exists between the narrow signals seen in two-photon experiments of this type and the narrow signals described in the previous sections. The two-photon signal arises from *all* molecules that absorb one photon from each of the counter-propagating beams, whereas the narrow signals described in the previous sections depend on the contribution of only one particular velocity component of the group of molecules to the signal.

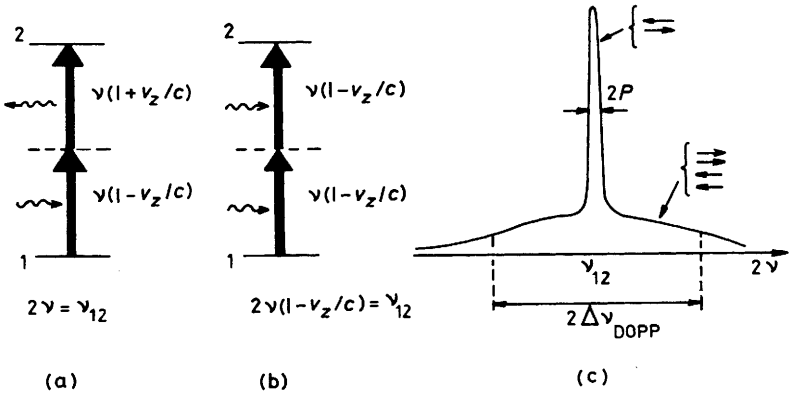

Figure 4 *(a) Compensation for the Doppler shift in the simultaneous absorption of two photons from two counter-running waves. (b) Absence of compensation from two unidirectional waves. (c) Shape of the narrow resonance in two photon absorption*

H. Optical-microwave Double Resonance.—A final way of reducing the Doppler broadening in the infrared and visible regions is to shift the detection from the optical to the microwave region, where the Doppler widths are very small. These double resonance methods involve either saturating the optical transition and detecting the effects of this on the microwave absorption, or *vice versa*. The

[13] V. S. Letokhov, *Science*, 1975, **190**, 344.
[14] V. S. Letokhov and V. P. Chebotaev, 'Nonlinear Laser Spectroscopy', Springer Series in Optical Science, Springer Verlag, Berlin, 1977, Vol. 4.

observation of double resonance signals requires either that the optical and microwave transitions share a common level, or that the levels are strongly coupled by collisions that obey well defined selection rules.

A variation of optical-microwave double resonance is two-photon spectroscopy, where the optical and microwave photons are absorbed simultaneously, so that the sum or difference of the frequencies of the optical and microwave photons is equal to the frequency of the transition being probed. Two-photon transitions have been observed in molecules subjected to a standing-wave field in which case 'two-photon Lamb dip' signals are seen. Since both the two-photon and the Lamb dip processes are non-linear in the radiation field, the theory is rather complicated.[15]

Several rather complete reviews of the subject matter of this section have recently appeared, and the reader is referred to them for further information.[16, 17]

3 Experimental Techniques

A. Resonance Methods.—Resonance methods that rely on 'tuning a molecule' rather than a laser were the first techniques to be developed for Doppler-limited and for saturation spectroscopy, since lasers with a good broadband tuning range were not available until the early 1970's. The first two methods to be developed relied on the use of electric or magnetic fields to tune a particular set of transitions into resonance with a stable fixed-frequency gas laser. These methods are known as 'Laser Stark Spectroscopy' in the case of electric field tuning, and 'Laser Magnetic Resonance', (LMR), when magnetic field tuning is used. Both methods suffer from the disadvantage that a conversion from field sweep to frequency has to be made. The position of the zero-field transition frequency must therefore be inferred from the field tuning pattern. Despite this drawback they are still widely used owing to their high sensitivity, particularly of LMR, which has led to the detailed study of a wide range of free radicals and semi-stable species.

Other resonance techniques that employ fixed-frequency lasers, or tunable lasers locked in frequency, are beam methods: ion-beam and bolometric spectroscopy. Both of these methods detect the absorption of radiation *via* some change in the properties of the ion or molecule, such as enhanced dissociation or heat capacity, rather than by detecting changes in the intensity of the radiation field itself.

(i) *Laser Stark Spectroscopy.* The use of electric modulation methods in spectroscopy dates from its introduction in microwave spectrometers in 1948.[18] These methods allow a considerable enhancement in signal to noise ratio over video detection methods, since the only signal detected is due to molecular modulation of the microwaves.

[15] F. Shimizu, *Phys. Rev. A*, 1974, **10**, 950.
[16] H. Jones, 'Modern Aspects of Microwave Spectroscopy', ed. G. W. Chantry, Academic Press, 1979, p. 123.
[17] T. Oka, 'Frontiers in Laser Spectroscopy', ed. R. Balian *et al.*, North Holland, 1977, p. 531.
[18] C. H. Townes and A. L. Schawlow, 'Microwave Spectroscopy', McGraw Hill, 1955.

In the infrared and visible regions it is possible to use parallel plate Stark cells in which very homogeneous electrostatic fields can be generated, and hence precise values of electrical properties of molecules, such as the dipole moment, can be measured. These methods were pioneered by Shimoda's Group in 1967,[19] and in their present form by Shimizu in 1970.[20,21] The original type of apparatus used a single CO_2 or CO laser, and this method of electric resonance spectroscopy has become known as Laser Stark Spectroscopy.

In laser Stark spectroscopy, fixed-frequency laser radiation is passed through a parallel plate Stark cell. At certain values of the applied electrostatic field-specific electric-field components of the molecular vibration–rotation, or pure rotation, transitions of the absorbing gas are brought into resonance with the laser frequency giving rise to an electric resonance spectrum. In microwave spectroscopy it is conventional to use a waveguide Stark cell in which the electric vectors of the static electric field and of the radiation field are parallel, giving rise to the selection rule $\Delta M_J = 0$. In the infrared region the short wavelength radiation propagates through the Stark cell as a free-space wave and hence the electric vector of the radiation field can be both parallel and perpendicular to the static electric field, leading to both $\Delta M_J = 0$ and $\Delta M_J = \pm 1$ selection rules in the observed spectra.

Since the method relies on the use of an electrostatic field for tuning, it is necessary to generate high uniform-fields and to study molecules with appreciable Stark tuning coefficients. In order to generate high electrostatic-fields, which may approach $90\,kV\,cm^{-1}$, narrow plate spacings of from 1 to 4 mm are commonly used. With such narrow gaps the plates must be flat to within one or two fringes of visible light, and be held accurately parallel. The gas pressure used must also be restricted to the low-pressure region below 100 millitorr. A useful rule of thumb is that a potential difference of 3000 volts may be sustained without electrical breakdown across any gas at a pressure of 10 millitorr and below. The Paschen curve of breakdown voltage against pressure for a particular gas can then be used to extrapolate to a different pressure/voltage regime. It should be noted that the minimum in the Paschen curve occurs at *ca.* 1 torr pressure, and hence that very restricted Stark tuning is available at higher pressures.

The detectors used are quantum limited liquid nitrogen cooled semiconductor devices, PbSnTe or CdHgTe in the 10 μm region and Au doped Ge in the 5μm region. Modulation frequencies of 5 to 100 kHz are used to get above the principal noise region of the 5 and 10 μm gas lasers.

Intracavity[22] or multiple-pass absorption cells of the Shimizu type[23] are generally used, as described in Section 2C. In both types of cell Lamb dips can usually be seen due to the presence of a standing-wave field. The main disadvantage of the

[19] K. Sakurai, K. Uehara, M. Takami, and K. Shimoda, *J. Phys. Soc. Jpn.*, 1967, **23**, 103.
[20] F. Shimizu, *J. Chem. Phys.*, 1970, **52**, 3572.
[21] F. Shimizu, *J. Chem. Phys.*, 1970, **53**, 1149.
[22] J. W. C. Johns and A. R. W. McKellar, *J. Chem. Phys.*, 1977, **66**, 1217.
[23] G. L. Caldow, G. Duxbury, and L. A. Evans, *J. Mol. Spectrosc.*, 1978, **69**, 239.

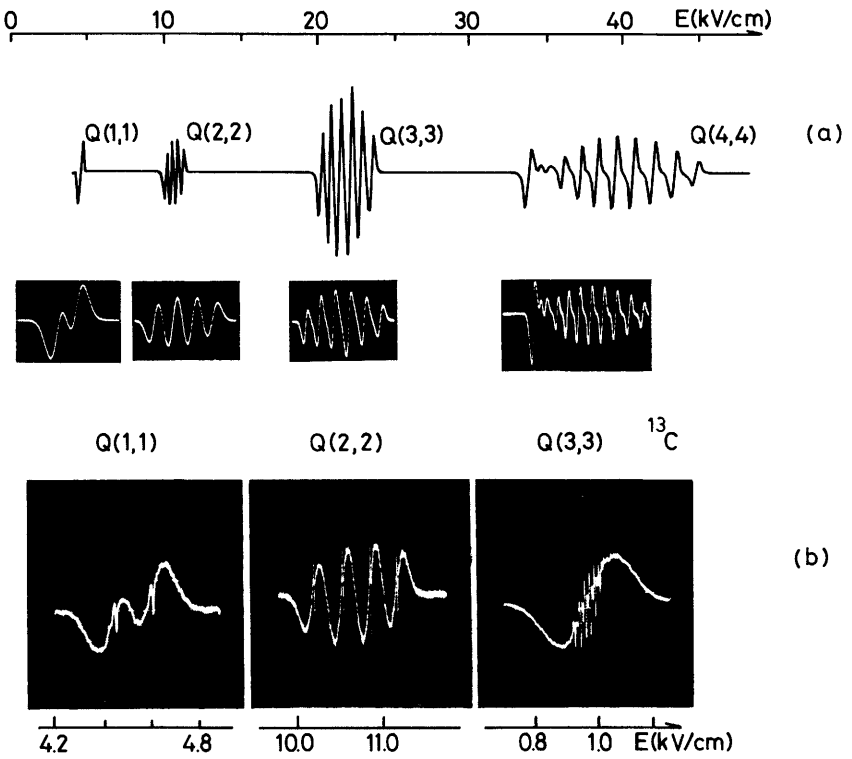

Figure 5 *(a) Observed $\Delta M = \pm 1$ transitions for the Q-branch series of $^{12}CH_3F$. The laser line used is the CO_2 9μm P(18) line. The upper trace is a computer calculated band contour and the lower picture shows observed oscilloscope traces. The features on the shoulder belong to the Q (3,2) pattern. The sample pressure was about* 5 m torr, *and the time constant for detection was* 10 ms. *(b) Q(1,1) and Q(2,2) and Q(3,3) in $^{13}CH_3F$ transitions with Lamb dip resolution* (Reproduced by permission from *J. Mol. Spectrosc.*, 1974, **53**, 38)

intracavity cells is that the spot size of most infrared gas lasers restricts their use to the 5 μm region, so that only low fields can be achieved as the plate spacings must be *ca.* 3 to 4 mm.

The transitions seen in the ν_3 band of CH_3F form a useful vehicle for discussion of typical laser Stark patterns.[24] The 9 μm P(18) line of the CO_2 laser lies very close to the ν_3 vibrational band origin. In perpendicular polarization the lowest J Q_Q transitions to be seen with $\Delta M_J = \pm 1$ selection rules are shown in Figure 5. The spectrum consists of a set of Q_Q transitions ($^{\Delta K}\Delta J$) which are brought into resonance at differing values of the static electric field. The first derivative shape is due to the use of small amplitude sinusoidal modulation, and is similar to that

[24] S. M. Freund, G. Duxbury, M. Romheld, J. T. Tiedje, and T. Oka, *J. Mol. Spectrosc.*, 1974, **38**, 52.

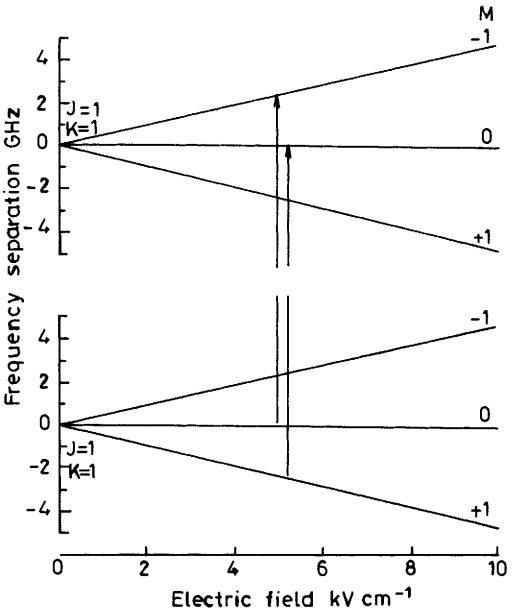

Figure 6 *Stark energy level diagram for the* $Q(1,1)$ *transition of* $^{12}CH_3$ *with* $\Delta M = \pm 1$. *Since the Stark shifts of the excited and ground states are very similar, the splitting of the* $Q(1,1)$ *resonance indicated in Figure 5 is caused by the small difference between the dipole moments in the upper and lower states of* CH_3F
(Reproduced by permission from *J. Mol. Spectrosc.*, 1974, **52**, 38)

observed in e.s.r. spectra.[25] The origin of the patterns can be seen using the energy level diagram of Figure 6. It can be seen that if the dipole moment of the molecule is the same in the two vibrational states, and if the Stark tuning approximates to first order, all the resonances for a particular vibration–rotation transition will be degenerate. Since the Stark effect in many of the rovibrational transitions of CH_3F is nearly first order, the centre of the patterns is determined by the average value of the dipole moment in the two states, and the spread of the pattern by the difference. The number of the components is given by $2J$, and hence gives the J value of the transition. It should be noted that if the conventional microwave arrangement of parallel polarization is used, these resonances are seen only at very high values of the electric field since the transitions then tune as the dipole moment difference, *ca.* 0.05 D. The rather asymmetric pattern of the ^QQ (3, 2) transition shows that at high values of the Stark field the second and higher order effects can be very important. This means that the usual perturbation treatment of the Stark effect[18] is inadequate for low J values, and that methods involving the diagonalization of truncated infinite matrices must be used in order to fit the spectra.[24]

[25] A. Carrington, 'Microwave Spectroscopy of Free Radicals', Academic Press, 1974.

The line widths observed in the spectra often provide clues to the assignment of spectra. If the Stark shifts are approximately first order, the apparent widths of the lines in terms of electric field are related to the Doppler width by the relationship

$$\Delta V/V = \Delta\nu_D/[\nu_{laser} - \nu_0] \quad (13)$$

where ΔV is the width of the resonance, and V is the central voltage. $\Delta\nu_D$ is the width between the points of maximum slope, $2\ \delta/\sqrt{2}$, and $[\nu_{laser} - \nu_0]$ is the frequency offset between the laser and the zero-field line. This relationship was particularly useful in the analysis of the spectrum of an unstable species such as HNO or H_2CS, where the conventional gas-phase spectrum had not been obtained at the time of the original analysis, and where the band origins were obtained from matrix isolation data at low resolution. Other characteristic patterns are found for P and R branches of parallel bands[25] and for Q branches of perpendicular bands.[26]

Even though the Doppler-limited spectra of light molecules such as NH_3 and CH_3F can often be resolved, it is frequently impossible to resolve the structure in the crowded regions of the spectrum. Indeed, with heavier molecules such as 1,1-difluoroethylene, CH_2CF_2, it becomes very difficult to find regions in which simple patterns can be clearly seen. The types of saturation spectroscopy discussion in Section 2 have been widely applied in Stark spectroscopy to give greatly enhanced resolution. This has enabled the structure of crowded spectral regions to be resolved, and has allowed the measurement of small changes in the electric dipole moments with vibrational states, as well as the measurement of small vibrationally or rotationally induced dipole moments, and the effects of weak intermolecular forces *via* the observation of four-level resonance signals.

B. Laser Magnetic Resonance Spectroscopy (LMR).—LMR relies on the same idea as laser Stark spectroscopy, namely the magnetic field tuning of specific Zeeman components of pure rotation or vibration–rotation transition into resonance with a fixed frequency laser. The apparatus is more bulky than the Stark system, since a large electromagnet is usually required to generate the magnetic field.

Since its introduction by Evenson and his colleagues in 1968[27] pure rotational LMR has proved to be one of the most powerful means of studying small paramagnetic species. The key to the success of the method was the adoption of the intracavity absorption cell pioneered by Wells and Evenson.[28] This allows the small changes in the absorption in the intracavity cell to be detected *via* the non-linear amplification of the laser medium, giving rise to a very long effective path length. The advantages of Zeeman spectroscopy over Stark spectroscopy stem principally from the restriction in pressure imposed in Stark cells, owing to the necessity of avoiding electric breakdown between plates, so that the pressure in the Stark cell is well below the optimum for radical production. The narrow gap

[26] G. Duxbury and S. M. Freund, *J. Mol. Spectrosc.*, 1977, **67**, 219.
[27] K. M. Evenson, H. P. Broida, J. S. Wells, R. J. Mahler, and M. Mizushima, *Phys. Rev. Lett.*, 1968, **21**, 1038.
[28] J. S. Wells and K. M. Evenson, *Rev. Sci. Instrum.*, 1970, **41**, 227.

between the plates also precludes routine intracavity operation of Stark cells, except in the 5 μm region. Finally there is the destruction of the species on the surface of the Stark plates. Intracavity Zeeman spectrometers resemble the Stark system of Figure 11a if the Stark plates are replaced by a magnet.

In general the energy level patterns seen in LMR spectra are more complex than their electric field equivalents, mainly as a result of two additional complications: the interplay of the various magnetic moments associated with the unpaired electron and the nuclear spins, and the effects of spin-uncoupling at high magnetic fields, the Paschen–Back effect. This is illustrated in Figure 7. At low field the angular momentum associated with the unpaired electron is tightly coupled to the nuclear frame and hence J and F are good quantum numbers. At the low-field limit the magnetic sub-levels of the vibration–rotation or pure rotation transition have different tuning rates, resulting in a differential tuning into resonance similar to that discussed for Stark spectra. However, when the electron spin is uncoupled from the nuclear frame at high fields, the main tuning observed is that of the free electron and the differential tuning is lost. This limits the molecules with large Zeeman tuning coefficients to those with large spin–rotation interaction constants, such as NH_2.[29] The spin–rotation interaction is responsible for the large zero-field splitting seen in Figure 7. Thus in LMR the spin–rotation constants, principally ε_{aa}, play an analogous role to the electric dipole moment μ in Stark spectroscopy in determining the tuning range, since ε_{aa} represents the magnetic moment about the a-axis which tends to align the spin with the molecular frame. LMR has a final and more subtle advantage over Stark spectroscopy in that the magnetic field does not mix levels of opposite parity, and hence information about asymmetry splitting in near prolate asymmetric tops such as H_2CS and HO_2 that is often lost in Stark spectroscopy, is preserved in LMR.

In pure rotation LMR the original lasers used, electric discharge HCN and H_2O devices, have largely been replaced by optically pumped lasers. In the mid-infrared region CO_2 and CO lasers are mainly used, in general with intracavity LMR cells.
(i) *Ion Beam Spectroscopy*. Much of the highest resolution ion-beam spectroscopy is carried out using fixed frequency lasers as described in a recent review by Carrington.[30] It is a resonance technique in that the molecules are tuned into resonance with the laser, but it differs from LMR and laser Stark spectroscopy in that direct Doppler tuning of the molecular ion is accomplished by changing the ion velocity through the potential applied to a drift tube. The ions are generated in a mass spectrometer source giving a beam flux of $10^{10} - 10^4\ s^{-1}$, with an effective ion concentration of $10^4 - 10^6$ ions cm^{-3}. Light ions with a mass in the range 2 to 20, can be accelerated to a velocity of *ca.* $10^5\ ms^{-1}$ with an acceleration potential of a few k eV. In the drift tube the ion beam is colinear with that of a laser, which is reflected so that positive and negative Doppler shifts can be employed. Detection of the absorption of radiation is observed by modulating the laser beam and

[29] P. B. Davies, D. K. Russell, B. A. Thrush, and H. E. Radford, *Proc. R. Soc. London, Ser. A*, 1977, **353**, 299.

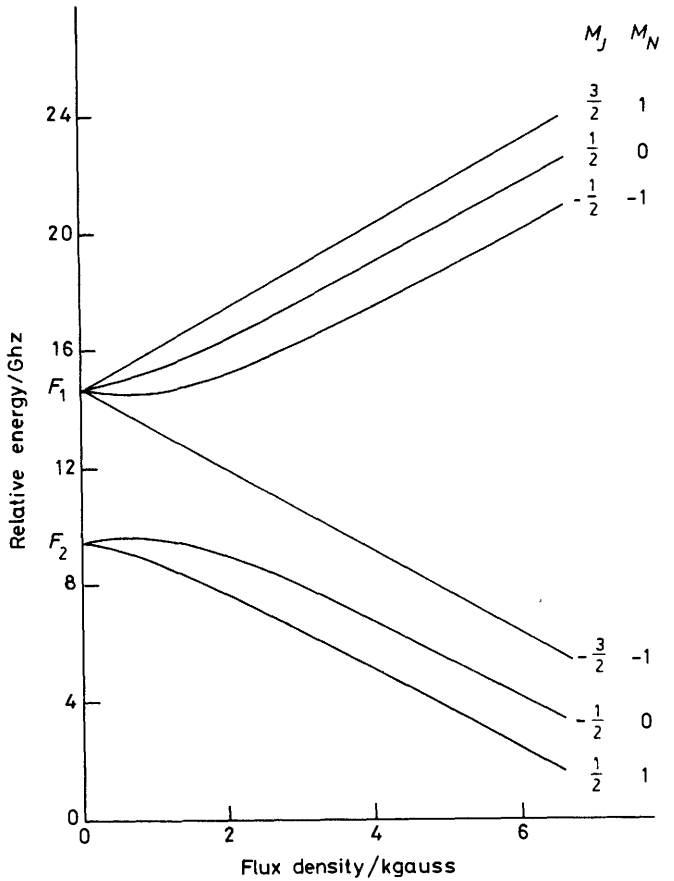

Figure 7 *Electron spin uncoupling in the levels of a polyatomic molecule caused by application of an external magnetic field (the Paschen–Back effect). At low fields the spin is coupled to the molecular frame and the Zeeman splitting is linear in M_J. At high field, spin is oriented with respect to the magnetic field direction in the laboratory frame, and the Zeeman splitting is linear in M_S. The lower set of levels correspond to $M_S = -\frac{1}{2}$, and the upper set to $M_S = +\frac{1}{2}$. Note that $M_J = M_N + M_S$*
(Reproduced by permission from 'Chemical and Biological Applications of Lasers', ed. C. B. Moore, Academic Press, 1980, p. 95)

detecting the effect of this on some property of the ions that changes with excitation. The three methods most commonly employed have been charge exchange, predissociation, and multiphoton-dissociation.[30]

One of the virtues of the ion beam method is that very high resolution is obtained owing to the kinematic compression of the velocity spread. This arises because

[30] A. Carrington, *Proc. R. Soc. London, Ser. A*, 1979, **367**, 43.

although the energy dispersion of the ions when formed is several tenths of an electron volt, this forms a small proportion of the total energy once the ion beam has been accelerated with an energy of a few kilovolts, and hence there are very large reductions in the Doppler width. The observed Doppler widths range from 10 MHz in the infrared to 100 MHz in the visible.

(ii) *Bolometric Spectroscopy.* In this method the infrared spectrum of a molecular beam is obtained using a 2 K doped silicon bolometer to measure the energy imparted to the beam by an appropriately tuned infrared laser,[31] or by tuning the energy levels of the molecules in the beam using the Stark effect.[32] This is a very sensitive method for obtaining accurate spectroscopic data on stable molecules and Van der Waals' clusters.

(iii) *Optical–Optical Double Resonance and Level Crossing.* As we saw in Section 2, if a molecular energy level splitting is tuned by the Stark or Zeeman effect, a non-linear response occurs for the resonance condition, $\Delta\Omega = \Delta\nu$, where $\Delta\Omega = \Omega_1 - \Omega_2$, the difference frequency between the laser beams co-propagating through the cell, and $\Delta\nu = \nu_1 - \nu_2$ is the difference frequency between the coupled transitions that share a common energy level. In the earliest experiments, carried out by Brewer,[9] two very stable CO_2 lasers were used to generate $\Delta\Omega$. However, it was subsequently realised that the use of a single-amplitude modulated laser removed the requirement for frequency locking two separate lasers, and also allowed the frequency difference to be set directly, as it corresponds to the frequency of the modulator radiofrequency drive oscillator. As the sidebands move in phase with the carrier, the difference frequency is independent of the frequency drift of the laser, depending only on the stability of the RF drive oscillator. Two methods have been used, electro-optic[33] and acousto-optic modulation.[34] Although electro-optic modulation was the first technique to be used to study the dipole moments of polar and non-polar molecules,[33] acousto-optic modulation produces a single sideband only and hence will be used in the following discussion. A block diagram of a single sideband OODR spectrometer is given in Figure 8. By use of a half-wave plate/linear polarizer combination, overall selection rules of ΔM_J (or ΔM_F) $= 0, \pm 1, \pm 2$ can be produced. For the selection rule $|\Delta M_J| = 2$, either beam 1 excites $\Delta M_J = +1$ and beam 2 $\Delta M_J = -1$, or *vice versa*. The resonance condition for a symmetric rotor is[34]

$$\Delta\Omega = \Omega_{RF} = \frac{2\mu EK}{hJ(J+1)} \tag{14}$$

If the overall selection rule is $|\Delta M_J| = 1$, the resonance condition for a symmetric rotor becomes

$$\Omega_{RF} = \frac{\mu EK}{hJ(J+1)} \tag{15}$$

[31] T. E. Gough, R. E. Miller, and G. Scoles, *Faraday Discuss. Chem. Soc.*, 1981, **71**, 77.
[32] T. E. Gough, personal communication.
[33] B. J. Orr and T. Oka, *Appl. Phys.*, 1980, **21**, 293.
[34] D. J. Bedwell and G. Duxbury, *Chem. Phys.*, 1979, **37**, 445.

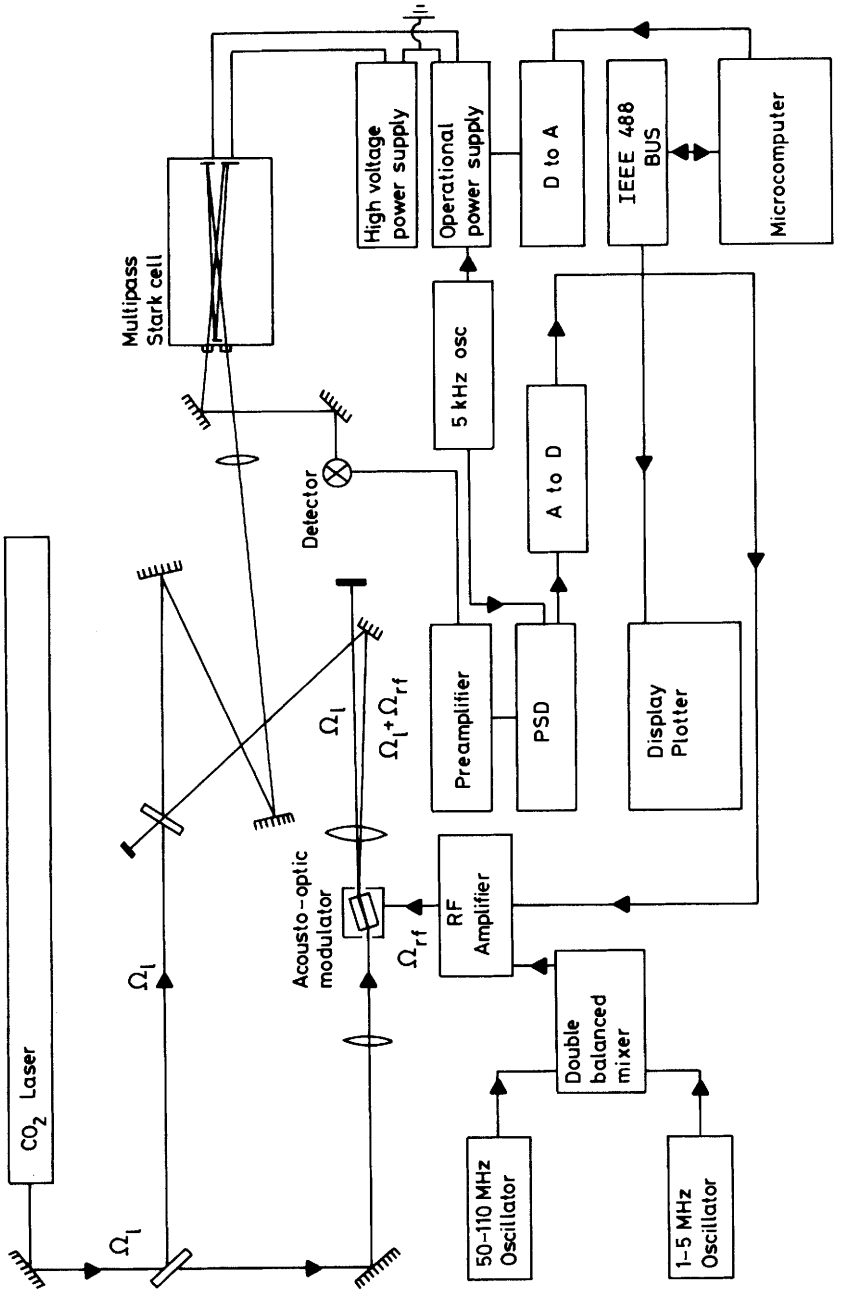

Figure 8 *Block diagram of a microcomputer controlled OODR spectrometer*

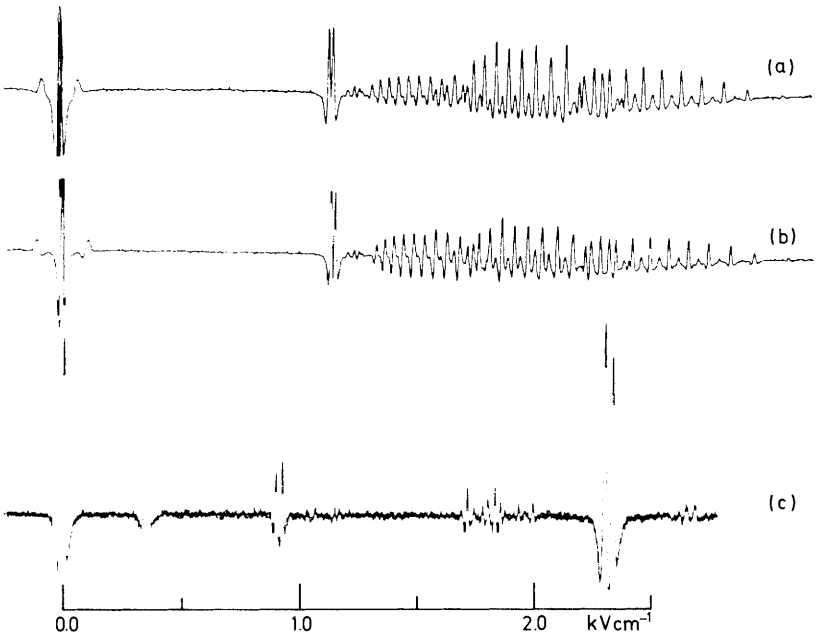

Figure 9 *OODR spectra of* CH_3OH *using the P(34) laser line of* CO_2. *(a) Two beams perpendicularly polarized, detecting in perpendicular polarization. (b) One beam perpendicular and one parallel polarized, detecting in perpendicular polarization. (c) As (b) but detecting in parallel polarization*

When the double resonance is carried out in a multiple-pass cell, signals due to Lamb dips and three- or four-level velocity tuned double resonances can be seen as well as the OODR signals. An example of these signals in CH_3OH is shown in Figure 9, where the use of polarization selective detection has allowed the removal of the unwanted standing wave signals.

If the second-order Stark effect is important,[35-38] the degeneracy of the M components of the double resonance signal can be broken, and resolved M structure seen. Similar effects can arise in electric resonance OODR when a quadrupolar nucleus is present.[34]

One of the limitations of acousto-optic modulators is that their drive frequencies are rather high and may therefore be too high to study species with small dipole moments. This can be overcome by the amplitude-modulated sideband method[38] in which the carrier is suppressed and the effective RF frequency is twice that of the amplitude modulation.

[35] B. J. Orr and T. Oka, *J. Mol. Spectrosc.*, 1977, **66**, 302.
[36] G. Duxbury, H. Kato, and D. Robinson, *J. Mol. Struct.*, 1982, **80**, 371.
[37] G. Duxbury, H. Kato, M. L. Le Lerre, J. McCombie, and J. C. Petersen, in 'Quantum Electronics and Electro-Optics', ed. P. L. Knight, Wiley, 1983, p. 191.
[38] G. Duxbury and H. Kato, *Chem. Phys.*, 1982, **66**, 161.

This method of double resonance, using a modulated source, is related to a method introduced by Dodd and Series[39] called 'resonances in a modulated light beam'. This is usually carried out using a weak light source and detecting the change in polarization of the emitted fluorescence as in the spontaneous emission level crossing experiments. The main difference from the experiments described above is that the detection is made at the RF beat frequency in the detector, as has been described by Lehman.[40] This requires a detector with a wide bandwidth, (up to 30 MHz has been used), whereas in the experiments described in this article, a low modulation frequency of up to 100 kHz is used, putting a less severe constraint on the detector and the subsequent amplifier and associated electronics.

Finite field level crossing and anti-crossing experiments have been carried out using both Stark and Zeeman tuning. The positions of the crossings or the avoided crossing are determined, for example, by the ratio of dipole moment matrix elements to the quadrupole matrix elements in the signals seen in CD_3I, and are therefore outside the control of the spectroscopist. For this reason level crossing or anti-crossing is a less flexible tool than OODR, although it has been exploited successfully in several systems. In all these experiments the information obtained is the ratio of the electric dipole moment to the rotational hyperfine, or quadrupole splittings, or of the magnetic moment to the hyperfine constants. Experiments such as OODR are necessary to fix one or other of the variables so that absolute values of parameters can be obtained from these measurements.

C. Frequency Swept Experiments.—These methods have been coming into general use over the last ten years, mainly due to the development of diode lasers, which provide coverage of most of the infrared region from 16 to 3 μm, and the development of dye lasers covering much of the near infrared, visible, and near ultraviolet regions.[2] In the infrared region the main method used is absorption spectroscopy, since the spontaneous emission probability is low. In the visible and near ultraviolet regions, where the spontaneous emission probability is high, laser-induced fluorescence is the most sensitive method of detection. For molecules that do not readily fluoresce, indirect detection methods can be used. The most commonly used methods are the opto-acoustic and opto-galvanic effects.

(i) *Sources.* Most of the tunable laser sources commonly used, dye lasers, lasers based on non-linear frequency mixing, and semiconductor diode lasers have been described in some detail in a previous *Chemical Society Review*.[41] The main lasers which have been developed in the intervening period are colour-centre lasers and waveguide CO_2 lasers.

Colour-centre lasers using F_A(II) centres in KCl:Li and in RbCl:Li provide 10 mW of tunable single mode power in the 2.3—2.8 and the 2.5—3.3 μm regions.[42] Since these lasers are pumped by ion lasers in the same way as dye lasers,

[39] J. N. Dodd, G. W. Series, and M. T. Taylor, *Proc. R. Soc. London, Ser. A*, 1963, **273**, 41.
[40] J. C. Lehman, *Rep. Prog. Phys.*, 1978, **41**, 1609.
[41] J. K. Burdett and M. Poliakoff, *Chem. Soc. Rev.*, 1974, **3**, 293.
[42] A. S. Pine, 'New Techniques In Optical and Infrared Spectroscopy', ed. G. W. Series and B. A. Thrush, *Philos. Trans. R. Soc. London, Ser. A*, 1982, **307**, 481.

they exhibit considerable amplitude fluctuations arising from the fluctuations in the ion-laser output. A commercial version of this type of laser is available, but requires considerable skill in operation.

By constructing optical waveguides of high conductivity, materials such as beryllia, boron nitride or alumina, high pressure operation of CO_2 laser systems has become possible. These lasers are compact devices with power output of several watts. For high power operation their tuning range is restricted to *ca.* $\pm$ 250 MHz from line centre, but up to $\pm$ 1000 MHz can be obtained from short lasers in which output power has been sacrificed to obtain a wider tuning range. Very stable lasers of this type have been constructed for use in non-linear spectroscopy.

A detailed review of all of the sources mentioned above, and also of some potentially useful devices, has recently been given by Mooradian.[43]

(ii) *Optogalvanic and Opto-acoustic Spectroscopy.* In both of these techniques the absorption of laser radiation is detected as a change in the bulk properties of the medium. Opto-acoustic spectroscopic signals are obtained when internal excitation is degraded into translational energy to produce sound waves. If the source of radiation is chopped, an AC sound signal is detected by an intracavity microphone. One graphic example of the sensitivity of this method is the observation of the opto-acoustic spectrum of the electronic spectrum of H_2CS[44] in a 10 cm long cell. The original experiments using conventional long-path absorption spectroscopy with a high resolution grating spectrometer required a pressure/path-length combination at least a factor of 10^4 greater.[45] Opto-acoustic spectroscopy is now widely used for trace-gas analysis and is reasonably well understood theoretically.

The other indirect technique, optogalvanic spectroscopy, is also under active study but the basis of the effect is still the subject of some controversy, although its usefulness in some circumstances has been conclusively demonstrated.[46,47] Optogalvanic signals arise when the impedance of a low-pressure discharge changes in response to the absorption of laser radiation by an atomic or molecular species within the discharge. The laser optogalvanic (LOG) spectrum is recorded by scanning the wavelength of the laser probing a DC excited discharge and monitoring the change in current through the discharge tube. The main requirement is that the discharge generates as little electrical interference in the detection system as possible. In some cases radiofrequency excitation is more suitable than the direct current method and, in that case, the impedance changes are detected by the reaction of the oscillator.

(iii) *Optical–Optical Double Resonance using Fixed Frequency and Tunable Lasers.* One method of combining the virtues of tunable and fixed frequency lasers to achieve sub-Doppler double resonance has been demonstrated by Weber and Terhune.[48,49] They carried out Stark-tuned double resonance experiments using

[43] A. Mooradian, *Rep. Prog. Phys.*, 1979, **42**, 1534.
[44] R. N. Dixon, D. A. Haner, and C. R. Webster, *Chem. Phys.*, 1977, **22**, 199.
[45] R. H. Judge and G. W. King, *J. Mol. Spectrosc.*, 1979, **74**, 175.
[46] A. I. Ferguson, *Ref.* 44, p. 645.
[47] C. R. Webster and R. T. Menzies, *J. Chem. Phys.*, 1983, **78**, 2121.
[48] W. H. Weber and R. W. Terhune, *Optics Lett.*, 1981, **6**, 455.
[49] W. H. Weber and R. W. Terhune, *J. Chem. Phys.*, 1983, **78**, 6437.

a CO laser as a pump and a diode laser as a probe. For example, in the first series of experiments, the CO laser was locked to one of the Stark components of the aR_R (9, 9) ν_4 transition of NH_3, and the diode laser probed the aQ (9, 9) ν_2 line. Complex narrow sub-Doppler features were seen, line narrowing effects and collision-induced resonances. This method should be generally applicable to the wide range of systems which lie within the tuning range of CO_2 and CO lasers.

D. The Experimental Detection of sub-Doppler Signals. —Although the principles of sub-Doppler spectroscopy described in Section 2 apply equally to experiments carried out in the infrared and the visible wavelength regions, the methods used to detect the sharp resonant signals are usually rather different. In the infrared region the spontaneous emission probability of the excited state is usually rather low and hence the saturated absorption signal is detected *via* the change in the absorption coefficient. In the visible region, however, the spontaneous emission probabilities are usually quite large, and hence the saturation of the transition is often monitored *via* spontaneous emission from the excited-state energy levels. In level crossing and anti-crossing experiments the differences between experiments in the two regimes are more marked. Linear-level crossing and anti-crossing signals can be observed *via* fluorescence detection but cannot be observed in direct absorption. The signals observed *via* laser induced fluorescence can therefore be due to mixtures of the linear and non-linear signals, whereas in absorption only the non-linear, or stimulated, signals can be seen.

Another distinction that can be made in the detection of signals induced by the interaction of molecules with a standing wave field is whether the standing wave field is produced by a two-beam or a multiple-beam system. Two-beam systems are frequently used in electronic spectroscopy, a typical arrangement being shown in Figure (10a). The finite crossing angle of the beams results in an incomplete removal of the Doppler broadening, but the separation of the pump and the probe beams allows various tricks to be employed to enhance the selectivity of the system. Two of the most commonly employed are intermodulated fluorescence[50] and polarization spectroscopy.[51] In intermodulated fluorescence the pump and the probe beams are chopped at frequencies ω_1 and ω_2, the fluorescence signal at either the sum frequency $\omega_1 + \omega_2$ or the difference frequency $\omega_1 - \omega_2$ is detected. Since both the pump and the probe beams are necessary to detect the Lamb dip, only the dip is modulated at the sum or the difference frequency, the background being modulated at either ω_1 or at ω_2 is rejected by the phase-sensitive detection system. A similar scheme has been used to record intermodulated optogalvanic and opto-acoustic spectra.[46] In polarization spectroscopy experiments the pump beam is circularly polarized and the probe beam linearly polarized, as shown in Figure 10b. The circularly polarized beam induces an optical anisotropy in the sample, so that the atoms or molecules 'dressed' by the circularly polarized field rotate the plane

[50] M. S. Sorem and A. L. Schawlow, *Optics Commun.*, 1972, **5**, 148.
[51] C. Wieman and T. W. Hansch, *Phys. Rev. Lett.*, 1976, **36**, 1170.

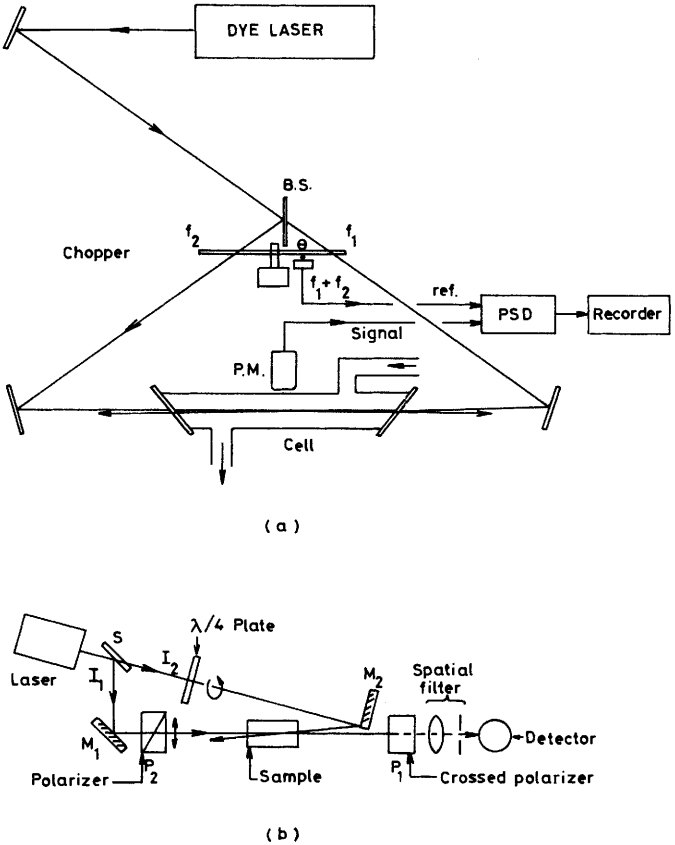

Figure 10 *Two-beam saturation spectroscopy arrangements. (a) Intermodulated fluorescence. (b) Polarization spectroscopy*
(Reproduced by permission from *Opt. Commun.*, 1972, **5**, 148; *Phys. Rev. Lett.*, 1976, **36**, 1170)

of polarization of the probe beam. The molecule interacting with a strong 'handed' field thus behaves like a chiral molecule and the rotated probe beam can then pass through the analysing polarizer, which is crossed for the original direction of linear polarization. Since only the molecules with $v_z = 0$ can be both pumped and probed in this way only Lamb dip signals are detected. Various versions of these methods such as polarization-intermodulated excitation, POLINEX, have been used subsequently.

In the infrared region the principal methods used for sub-Doppler spectroscopy have involved the use of multiple-beam systems. These consist of either multiple-pass cells in the Shimizu configuration[23] or intracavity cells.[22] These are shown in Figures 11a and 11b. An intracavity cell can be considered as an example of a

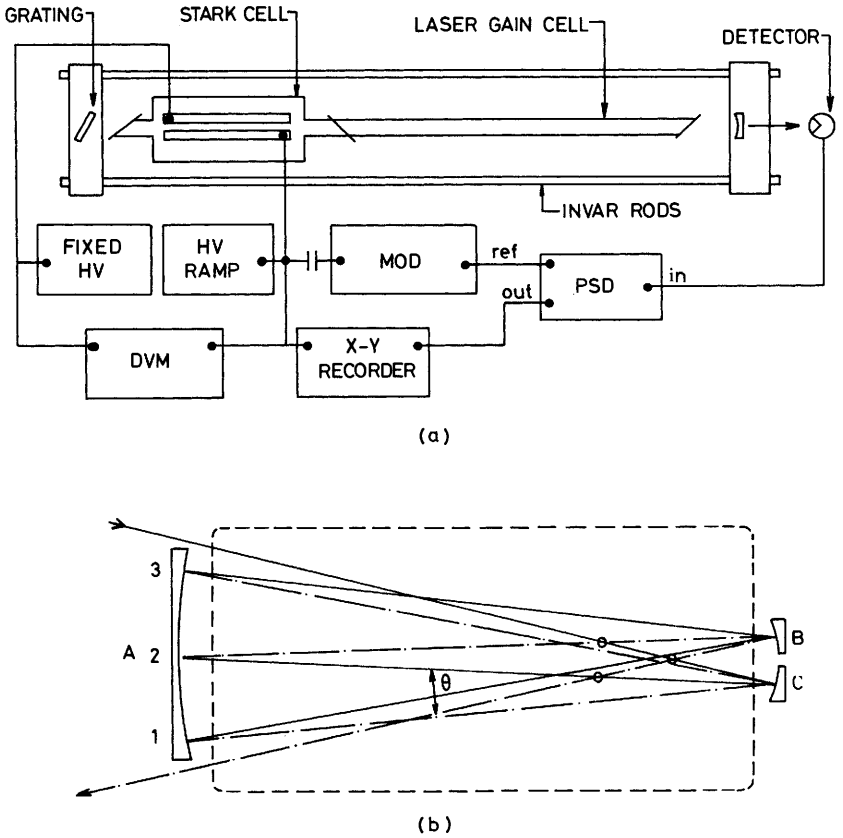

Figure 11 *(a) Schematic diagram of an intracavity laser Stark spectrometer. PSD stands for phase sensitive detector, DVM for digital voltmeter, HV for high voltage, and mod for modulation source*
(Reproduced by permission from *J. Chem. Phys.*, 1977, **66**, 1217)
(b) Mirror configuration of a crossover White's cell of the Shimizu type with N = 4. The solid lines show beams propagating from left to right, and the broken lines from right to left. The circules are the crossing points between solid and broken lines. The angle θ represents the finite crossing angle of the beams. The Stark electrodes are parallel to the paper and occupy the area shown by the broken line rectangle
(Reproduced by permission from *J. Mol. Spectrosc.*, 1978, **69**, 239)

multiple-beam system since the Fabry–Perot cavity of the laser acts as a multiple-pass system for the generation of the laser signal, and hence the absorber can be considered to affect the gain for each pass. In multiple-pass systems the forward and the backward waves are equal in intensity, and selective modulation of the pump and the probe beams is not practicable. However, the detection systems commonly used do in fact allow the sub-Doppler signals to be enhanced relative to the background. The main detection schemes use either a small amplitude electric or magnetic field modulation, or a small amplitude frequency modulation

of the laser. This results in the signal from the phase-sensitive detection system being detected as a derivative signal.[52] Since it is also possible to detect signals at harmonics of the modulation frequency, further selectivity is possible. Detection at the second harmonic of the modulation frequency results in a second derivative signal, which resembles an inverted absorption signal. Since the Doppler-broadened background is a slowly varying function of either field or frequency, second-derivative detection results in an almost complete suppression of the background if the modulation amplitude is of the order of magnitude of the linewidth of the sub-Doppler signal as is shown in Figure 9. Detection at the third harmonic is sometimes employed, particularly in laser stabilization systems. The third-derivative signal resembles a sharpened first-derivative signal but with far better background suppression. Third-derivative signals are, however, rather weak and hence the method is only suitable for molecules that are strong absorbers. Tests carried out with similar modulation methods in the visible region have shown that high frequency modulation methods give a signal to noise ratio that is only slightly inferior to that provided by methods such as intermodulated fluorescence. Multiple-beam cells are particularly useful for the detection of free radicals and of trace constituents since, for a limited volume cell, the total absorption coefficient is greatly enhanced over a two-pass system.

The final differences that we consider, between saturation spectroscopy in the infrared and the visible wavelength regions, depend upon the type of laser used. In the infrared region most of the tunable lasers that have been developed, in particular diode lasers, generate insufficient power for saturation experiments. Most experiments so far have therefore been carried out with CO or CO_2 lasers. These lasers are line tunable but possess only a limited frequency tuning range about the centre frequency of each emission line. Most of the sub-Doppler experiments therefore depend upon the use of resonance methods. In the visible region the principal lasers used are dye lasers, which do allow sufficient power to be generated for saturation experiments, hence most experiments are carried out in the frequency swept regime.

4 Stark Spectroscopy of Small Molecules

Stark spectroscopy has been used for two main purposes, as a high resolution spectroscopic method for measuring the absorption spectra of low pressure gases, particularly of short lived species, and for the accurate measurement of electric dipole moments.

It soon became evident that although the *absolute* precision of dipole moment determination by laser methods was little better than that achieved in the best microwave spectrometers, and was inferior to that of microwave molecular beam systems, the laser based spectrometers provided a more accurate wave of measuring *changes* in dipole moment than is possible in most microwave spectroscopy experiments. Furthermore, for some 'non-polar' molecules only laser techniques

[52] D. H. Whiffen, 'Spectroscopy', Longmans, 1966, p. 55.

were suitable for the measurement of the small vibrationally and rotationally-induced dipole moments. Most of the experiments so far have been carried out using fixed frequency, or frequency locked, lasers.

A. Electronic, Vibrational, and Rotational Dependence of Dipole Moments.—The variation of the dipole moment of a molecule with its state is associated with the distortion of the electronic charge distribution. For changes in the electronic state it is easy to visualise a large effect occurring. The best known examples of this are the large changes of dipole moment that have been measured in aldehydes, particularly formaldehyde, between the ground and the first excited state. These large changes are associated with the promotion of an electron from a non-bonding orbital to an antibonding π orbital on electronic excitation. The changes induced by vibration and rotation are usually much smaller, and are associated with the distortion of the nuclear frame from the equilibrium geometry. The formal treatment of these effects is similar to that applied to vibration–rotation interaction, where the vibrational and the rotational distortion effects are observed *via* the vibrational dependence of the rotation constants and the need to invoke centrifugal distortion constants.

(i) *Vibrational Effects.* The dipole moment of a polyatomic molecule may be expanded as a power series in the vibrational quantum numbers, and to first order in v may be written as

$$\mu = \mu_e + \sum_s \delta\mu_s v_s \tag{16}$$

where μ_e is the equilibrium dipole moment and v_s is the vibrational quantum number of the s'th normal mode. Two terms contribute to $\delta\mu_s$, one involving first derivatives of the dipole moment with respect to changes in the vibrational co-ordinates, and one involving the second derivative with respect to the s'th co-ordinate, *e.g.* for the ν_3 vibration of CH_3F, the CF stretching vibration, $\delta\mu_3$ takes the form[24,53]

$$\delta\mu_3 = -\left[\frac{k_{133}}{\nu_1}\left(\frac{\partial\mu}{\partial q_1}\right) + \frac{k_{233}}{\nu_2}\left(\frac{\partial\mu}{\partial q_2}\right) + \frac{3k_{333}}{\nu_3}\left(\frac{\partial\mu}{\partial q_3}\right) + \tfrac{1}{2}\left(\frac{\partial^2\mu}{\partial q_3^2}\right)\right] \tag{17}$$

where ν_3 and k_{333} *etc.* are the vibration frequencies and cubic anharmonic force constants, q_s is the s'th normal co-ordinate (in dimensionless units).

It should be noted that the sum only includes the dipole moment derivatives for totally symmetric vibrations in the case of C_{3v} molecules such as CH_3F, and for the in plane vibrations for C_{2v} molecules such as H_2CO.

A number of problems arise in the comparison of the experimentally determined dipole moment variations with those expected on the basis of the theory presented above. In very few molecules is the anharmonic force-field well determined, nor is the absolute sign of the $\partial\mu/\partial q_s$ known in most cases, since the observables are the

[53] M. Toyama, T. Oka, and Y. Morino, *J. Mol. Spectrosc.*, 1964, **13**, 193.

infrared intensities, which depend upon the square of the dipole moment derivative. However, it is often possible, by the use of simplified models[24,54] and of information on the intensity asymmetry of Coriolis coupled vibration–rotation bands,[55] to obtain some insight into the reasons for the patterns of dipole moment variation found.

One of the most interesting effects of dipole moment variation occurs in molecules such as methane. At its equilibrium geometry it posesses no electric dipole moment, but under the influence of non-totally symmetric vibrations the 'vibrationally averaged' dipole moment is non-zero. This means that the 'vibrationally' averaged structure is no longer tetrahedral, a type of vibrational Jahn–Teller effect. The original model, which was due to Mizushima and Venkateswarlu,[56] has been extended by Mills *et al.*[57]

Vibrational changes in the electric polarizability tensor are also associated with the size of the dipole moment derivatives. However, unlike the changes in dipole moment mentioned above, the polarizability changes are directly related to the infrared intensities, *i.e.* to the square of the derivatives. Changes in the polarizability are usually difficult to measure, as the polarizability plays a very minor role in the Stark shifts seen in most spectra. They have recently been observed in CO_2 which has no permanent dipole moment.[58]

(ii) *Rotational Effects.* The theory of the rotational dependence of dipole moments is, in its present form, largely due to Watson.[59,60] The effect can be most easily visualized as caused by the centrifugal distortion affecting the geometrical structure. This effect can be expressed as:

$$[\delta\mu_\alpha]_{\text{cent}} = \Sigma_k \left[\frac{\partial\mu_\alpha}{\partial Q_k}\right][\delta Q_k]_{\text{cent}} \tag{18}$$

where the Q_k are the normal co-ordinates. In the molecule fixed co-ordinate system, the dipole moment can be written as:

$$\mu_\alpha = \mu_\alpha^{(e)} + \Sigma_{\beta\gamma}\,\theta_\alpha^{\beta\gamma} J_\beta J_\gamma \tag{19}$$

where J_α, the molecule-fixed components of the total angular momentum, are in units of h, and the coefficient of the dipole moment, $\theta_\alpha^{\beta\gamma}$, which is in units of electric dipole moment is given by:

$$\theta_\alpha^{\beta\gamma} = \theta_\alpha^{\gamma\beta} = 2\Sigma_k \left[\frac{B_\beta B_\gamma}{\omega_k^2}\right]\left[\frac{\partial I_{\beta\gamma}}{\partial Q_k}\right]\left[\frac{\partial\mu_\alpha}{\partial Q_k}\right]_e \tag{20}$$

[54] G. Duxbury, S. M. Freund, and J. W. C. Johns, *J. Mol. Spectrosc.*, 1976, **62**, 99.
[55] C. di Lauro and I. M. Mills, *J. Mol. Spectrosc.*, 1966, **21**, 386.
[56] M. Mizushima and P. Venkateswarlu, *J. Chem. Phys.*, 1953, **21**, 705.
[57] I. M. Mills, J. K. G. Watson, and W. L. Smith, *Mol. Phys.*, 1969, **16**, 329.
[58] T. E. Gough, B. J. Orr, and G. Scoles, *J. Mol. Spectrosc.*, 1983, **99**, 143.
[59] J. K. G. Watson, *J. Mol. Spectrosc.*, 1971, **40**, 536.
[60] J. K. G. Watson, unpublished notes.

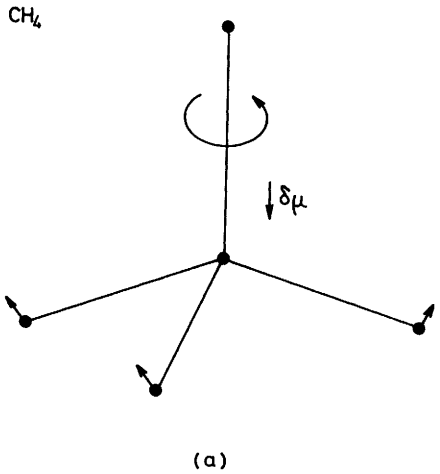

Figure 12 *Centrifugal distortion-induced dipole moment in* CH_4
(Reproduced by permission from 'Molecular Spectroscopy: Modern Research', ed. K. N. Rao, Academic Press, 1976, II.)

where B_β is the rotational constant for the β-axis, and $\partial I_{\beta\gamma}/\partial Q_k$ is the distortion of the $\beta\gamma$ component of the inertia tensor with the excitation of the k^{th} vibrational mode, which is of frequency ω_k.

From the above it can be seen that in order to calculate the vibrational and the rotational changes in dipole moment it is necessary to have a detailed knowledge of the changes in the dipole moment associated with excitation of particular normal vibrational modes in a molecule.

The most interesting effect of rotational distortion is probably the production of a rotationally induced dipole moment in non-polar molecules, particularly those of tetrahedral equilibrium geometry. The distortion of a tetrahedral frame needed to produce such an induced moment is shown in Figure 12. Examples of both vibrationally and rotationally induced changes in dipole moment will be given in the following sections.

B. Experimental Measurement of Dipole Moment Variation.—(i) *Vibrational and Rotational Dependence in Polar Molecules.* The dipole moment variation with vibrational state has been studied in some detail for three small polyatomic molecules, ammonia, methyl fluoride, and formaldehyde. In some of these molecules there is also some evidence for a rotational dependence of the dipole moment.

Ammonia was the first molecule to be studied by laser Stark spectroscopy.[20,21] It was discovered that a very large change in dipole moment, 0.22 D, occurred on the excitation of one quantum of the bending vibration, v_2, and that there was some indication of a rotational dependence of the dipole moment as well.[61] Since the

[61] K. Shimoda, Y. Ueda, and J. Iwahori, *Appl. Phys.*, 1980, **21**, 181.

inversion barrier in ammonia is rather low, about two vibrational quanta of v_2, a large change in dipole moment is to be expected, since if ammonia were planar the dipole moment would be zero. Since ammonia is inverting very rapidly, the 'dipole moment' of a state is really the expectation value of the dipole moment operator connecting the two components of an inversion doublet. Above the barrier to planarity the inversion doubling eventually becomes equal to half the vibrational spacing, and hence for high vibrational levels the vibrational spacing appears to be halved. Once the inversion doubling approaches the size of the vibrational spacing the vibrational transition moment and the 'dipole moment' become almost identical. This has been demonstrated by a recent experimental study of the $2v_2 - v_2$ band of NH_3,[62] and by observations of the $2v_2$ band by Doppler free two photon spectroscopy.[63] Another set of recent measurements on NH_3[64] have shown some of the pitfalls in the laser Stark approach. The effective dipole moments of some of the inversion levels of the v_4 state of ammonia were measured. v_4 lies close to $2v_2$ and many of the levels are coupled *via* Coriolis interaction. One set of levels of the v_4 state is not coupled to levels of the $2v_2$ state, and the effective dipole moment of these levels is within 1% of that of the vibrational ground state. This is as expected from the theory of vibrational changes in dipole moment given previously since v_4 is a perpendicular vibration, and hence should produce little effect on the average value of the dipole moment along the symmetry axis. The other levels are strongly coupled and the 'dipole moments' measured ranged from 0.793 D to 1.326 D, compared with a ground state dipole moment of 1.47 D. The laser Stark method is therefore only really suitable for studies of unperturbed states where the molecular dipole moment can be treated as almost constant.

Methyl fluoride was one of the first molecules to be studied at both Doppler limited and sub-Doppler resolution. A series of measurements using both the laser Stark and OODR methods,[24,26,38,54] tied to the accurately known dipole moment of the ground state, has allowed the variation of the dipole moment to be measured in some detail. It has also allowed the isotopic dependence in the series $^{12}CH_3F$, $^{13}CH_3F$, and $^{12}CD_3F$ to be established. The results are summarized in Table 1. It can be seen that the dipole moment change on excitation of the v_3 vibration of CD_3F is approximately half that in CH_3F. This has been explained by a 'vibrational mixing' model.[54] A small rotational dependence of the dipole moment has also been established.[24]

Formaldehyde, H_2CO, is possibly the best characterized of the systems, since the dipole moment has been measured in almost all of the vibrational states of H_2CO, and in many of those of D_2CO, using CO and CO_2 laser Stark spectroscopy.[65-67] The dipole moments in excited vibrational levels involving v_2 and v_4 have been measured *via* the electronic spectrum, using the stimulated emission PUMP and

[62] M. Takami, H. Jones, and T. Oka, *J. Chem. Phys.*, 1979, **70**, 3557.
[63] W. K. Bischel, P. J. Kelly, and C. K. Rhodes, *Phys. Rev. A*, 1976, **13**, 1829.
[64] W. H. Weber and R. W. Terhune, *J. Chem. Phys.*, **78**, 6422.
[65] J. W. C. Johns and A. R. W. McKellar, *J. Chem. Phys.*, 1975, **63**, 1682.
[66] M. Allegrini, J. W. C. Johns, and A. R. W. McKellar, *J. Mol. Spectrosc.*, 1977, **67**, 476.
[67] D. Coffey, C. Yamada, and E. Hirota, *J. Mol. Spectrosc.*, 1977, **64**, 327.

Table 1 *Dipole moments* (D) *of* CH_3F, $^{13}CH_3F$, *and* CD_3F

	$^{12}CH_3F$	*Ref.*	$^{13}CH_3F$	*Ref.*	$^{12}CD_3F$	*Ref.*
ground state	1.8585(5)	*a*	1.8579(6)	*b*	1.8702(21)	*c*
v_3	1.9054(6)	*b*	1.9039(6)	*b*	1.8964(15)	*c*
v_5					1.8751(21)	*e*
v_6	1.859(5)	*f*			1.8771(7)	*d*
$2v_3$	1.9519(20)	*b*	1.951(4)		1.9170(5)	*e*
$v_3 + v_6$	1.909(5)	*f*			1.932(7)	*f*

[a] M. D. Marshall and J. S. Muenter, *J. Mol. Spectrosc.*, 1980, **83**, 279. [b] S. M. Freund, G. Duxbury, M. Romheld, J. T. Tiedje, and T. Oka, *J. Mol. Spectrosc.*, 1974, **52**, 38. [c] G. Duxbury, S. M. Freund, and J. W. C. Johns, *J. Mol. Spectrosc.*, 1976, **62**, 99. [d] G. Duxbury and S. M. Freund, *J. Mol. Spectrosc.*, 1977, **67**, 219. [e] G. L. Caldow and G. Duxbury, *J. Mol. Spectrosc.*, 1981, **89**, 93. [f] G. Duxbury and H. Kato, *Chem. Phys.*, 1982, **66**, 161.

Table 2 *Dipole moments (Debyes) for formaldehyde and thioformaldehyde in various vibrational and electronic states*

State		H_2CO	*Ref.*	H_2CS	*Ref.*
$^1A_1$	*ground state*	2.3315(5)	*a*	1.6491(4)	*a*
	$v_3 = 1$ (CS) $v_2 = 1$ CO	2.3470(5)	*b*	1.6576(12)	*c*
	$v_4 = 1$	2.3086(5)	*a*	1.622(3)	*e*
	$v_6 = 1$	2.3285(5)	*a*	1.642(5)	*e*
	$v_3 = 1$ (CO)	2.3250(25)	*d*		
	$v_5 = 1$	2.2844(47)	*d*		
	$v_2 = 2$	2.3605(20)	*d*		
	$v_2 = 4$	2.2723(86)	*f*		
	$v_2 = 2$ $v_4 = 2$	2.3222(47)	*f*		
	$v_2 = 1$ $v_4 = 4$	2.2825(33)	*f*		
$\tilde{a}\ ^3A_2$		1.29(3)	*g*		
$\tilde{A}\ ^1A_2$		1.56(7)	*g*	0.79(4)	*c*

State		D_2CO	*d*	D_2CS	*e*
$^1A_2$	*ground state*	2.3471(5)		1.658(3)	
	$v_3 = 1$ (CS) $v_2 = 1$ (CO)	2.3672(15)		1.661(3)	
	$v_3 = 1$ (CO)	2.319(10)			
	$v_6 = 1$	2.347(4)			

[a] B. Fabricant, D. Krieger, and J. S. Muenter, *J. Chem. Phys.*, 1977, **67**, 1576. [b] C. Brechignac, J. W. C. Johns, A. R. W. McKellar, and M. Wong, *J. Mol. Spectrosc.*, 1982, **96**, 353. [c] D. J. Bedwell and G. Duxbury, *J. Mol. Spectrosc.*, 1980, **84**, 531. [d] M. Allegrini, J. W. C. Johns, and A. R. W. McKellar, *J. Mol. Spectrosc.*, 1977, **67**, 476. [e] G. Duxbury, H. Kato, and M. L. Le Lerre, *Faraday Discuss. Chem. Soc.*, 1981, **71**, 97. [f] P. H. Vaccaro, J. L. Kinsey, R. W. Field, and H. L. Dai, *J. Chem. Phys.*, 1983, **78**, 3659. [g] R. N. Dixon and C. R. Webster, *J. Mol. Spectrosc.*, 1978, **70**, 314.

DUMP scheme of Field in a Stark-tuned system.[68] The dipole moment variation with v_4 is much larger than would usually be expected for an out of plane vibration because of the large amplitude motion in this particular co-ordinate. The changes

[68] P. H. Vaccaro, J. L. Kinsey, R. W. Field, and H. L. Dai, *J. Chem. Phys.*, 1983, **78**, 3659.

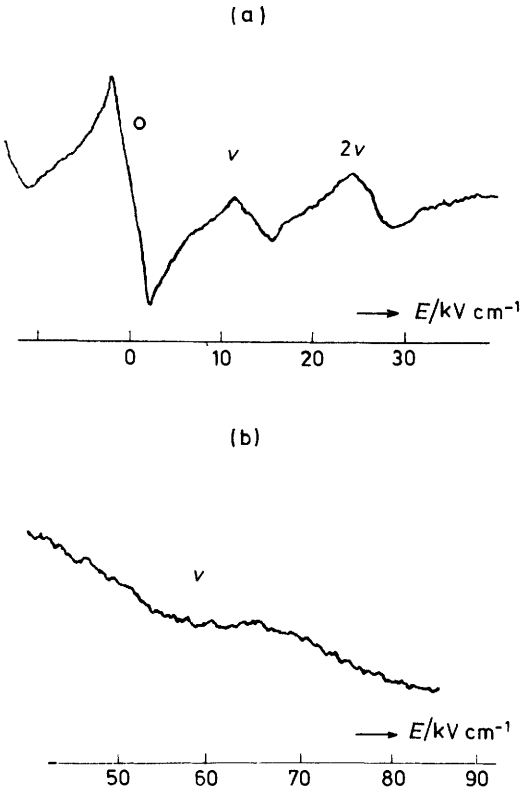

Figure 13 *OODR signals in* CH_3D *using electro-optic modulation. The resonances labelled* 2v *occur between the sidebands only, and those by* v *between the sidebands and the carrier. The polarizers are set so that both signals can be observed. (a) Signals due to the first-order Stark shift of the* $J = 9$, $K = 2$ *level of the* v_6 *state,* $\Omega_{RF} = 1.139$ MHz, $P = 4$ m torr. *(b) Signals due to the first-order Stark shift of the* $J = 10$, $K = 1$ *level in the ground state,* $\Omega_{RF} = 0.5722$ MHz, $P = 4$ m torr
(Reproduced by permission from *J. Chem. Phys.*, 1979, **70**, 5376)

in dipole moment are attributed to the smaller vibrationally projection of the CO and CH bond moments in the bent configuration upon the planar molecule configuration. The dipole moment variation in the other states is similar to that seen in CH_3F, with the main change being associated with the excitation of the CO stretching mode, v_2. This latter change is almost identical in v_2 of D_2CO since the CO stretching mode is almost an 'isolated' vibration in formaldehyde, unlike the situation when methyl fluoride is deuterated. These data are summarized in Table 2.

(ii) *Dipole Moments of Non-polar Molecules.* The principal experimental work in this area has been by Oka and his colleagues.[69] They have studied the dipole

[69] T. Oka, 'Molecular Spectroscopy: Modern Research', ed. K. N. Rao, Academic Press, 1976, II, p. 229.

moments induced by rotation in the tetrahedral molecules SiH_4[70] and GeH_4[71] by a variety of methods including, infrared–microwave double resonance, optical–optical double resonance, and laser Stark–Lamb dip spectroscopy. The results from experiments on the latest molecule in the series, CH_3D, will be described in some detail, since they exemplify many of the important aspects of the work. CH_3D has a small dipole moment of *ca.* 5.6×10^{-3} D which is due to the breakdown of tetrahedral symmetry. In order to observe OODR spectra very small RF frequencies and very high values of the applied electrostatic field are required as shown in Figure 13.[72] In a C_3v molecule there are only four independent θ parameters, $\theta_\zeta^{\xi\xi}$, $\theta_\zeta^{\zeta\zeta}$, $\theta_\xi^{\xi\zeta}$, and $\theta_\xi^{\xi\xi}$, where ζ is taken along the C_3 axis, the ξ axis on a σ_v plane and the η axis is perpendicular to them. Since the Stark effect depends upon the projection of the molecule fixed axes *onto axes fixed in the laboratory*, the space fixed axes, only certain linear combinations of the θ parameters are determined. The matrix elements which give rise to the first-order Stark shift are obtained by calculating the expectation value of the dipole moment operator in the space fixed axis system. This gives rise to an 'effective dipole moment operator' of:

$$\mu_\zeta(J,K) = \mu_\zeta^{(0)} - \theta_\xi^{\xi\zeta} + \left[\theta_\zeta^{\xi\xi} + 2\theta_\xi^{\xi\zeta}\right]J(J+1) - \left[\theta_\zeta^{\zeta\zeta} - \theta_\zeta^{\xi\xi} - 2\theta_\xi^{\xi\zeta}\right]K^2 \qquad (21)$$

When the $\theta_a^{\beta\gamma}$ are expressed in terms of the internal co-ordinates S_m, rather than the normal co-ordinates, the parameters in CH_4 and CH_3D can be related. In particular it could be shown that the parameters of CH_3D could be predicted from those of CH_4, which can be represented by a single parameter, θ_z^{xy}.[59,73]

(iii) *Polarizability Changes in Non-polar Molecules.* A recent experiment on CO_2 has provided information on an important property, the vibrational dependence of the molecular polarizability tensor. An *F*-centre laser has been used to excite the $\nu_1 + \nu_3$ band of CO_2 at 3715 cm^{-1} in a supersonic nozzle beam and the laser Stark spectrum bolometrically detected.[58] In order to measure the Stark splitting, fields of up to 230 kV cm^{-1} were required. This is much higher than the fields used in 'conventional' Stark spectroscopy, where the maximum field rarely exceeds 80 kV cm^{-1}. Measurements of the Stark splittings of the $R(0)$ and $P(2)$ transitions have allowed the evaluation of the isotropic part, (α_n), and the anisotropic part, $(\Delta\alpha_n)$, of the static polarizability in both the excited ($n = v$) and the ground ($n = 0$) states. The direct observables are $\Delta\alpha_v/\Delta\alpha_0 = 1.021$,[8] $(\alpha_v - \alpha_0)/\Delta\alpha_v = 0.012$,[6] and $\Delta\alpha_v = 2.65\,A^3$.[18] The result for $\Delta\alpha_v$ is 12% greater than that predicted for the static polarizability anisotropy, and the reason for this is not well understood. The other parameters are well predicted by the model for the vibrational dependence of α which is discussed in detail by Gough *et al.*[58]

(iv) *Dipole Moment Variations with Electronic State.* The change in dipole moment with electronic excitation is expected to be large compared with most vibrationally induced effects. Dipole moment changes with electronic excitation were first mea-

[70] W. A. Kreiner, T. Oka, and A. G. Robiette, *J. Chem. Phys.*, 1978, **68**, 3236.
[71] W. A. Kreiner, B. J. Orr, U. Andresen, and T. Oka, *Phys. Rev. A.*, 1977, **55**, 2297.
[72] J. K. G. Watson, M. Takami, and T. Oka, *J. Chem. Phys.*, 1979, **70**, 5376.
[73] I. Ozier, *Phys. Rev. Lett.*, 1971, **27**, 1329.

sured using high resolution grating spectrographs and spectrometers,[74-76] but laser methods allow a much higher resolution to be achieved and hence higher precision. They also permit the characterization of perturbations *via* the changes in the effective dipole moment, as we saw in the vibrational example, *i.e.* NH_3.[64]

As an example of the use of laser methods for the measurement of dipole moment changes the visible OODR spectrum of HNO observed by Dixon and his colleagues will be used.[77] They measured the Stark effect of several transitions in the $\tilde{A}^1A''$—$\tilde{X}^1A'$ spectrum of HNO using OODR with fluorescence detection. The tunability of the dye laser was exploited to select the desired zero-field coincidences, rather than the chance method using fixed frequency lasers. The amplitude modulation of the RF carrier by a second RF oscillator produced frequencies of $\Omega_L - \Omega_C \pm \Omega_M$, where Ω_L, Ω_C, and Ω_M are the frequencies of the laser, carrier, and modulator respectively. Thus the double resonance was between $\Omega_L - \Omega_C \pm \Omega_M$ and Ω_L, or between $(\Omega_L - \Omega_C) + \Omega_M$ and $(\Omega_L - \Omega_C) - \Omega_M$, with Ω_L suppressed. As Ω_M can be made very small, continuous tuning at low frequency can be achieved. Examples of the M resolved double resonance produced in this way are shown in Figure 14.

As the ground state of HNO has been studied in some detail by laser Stark spectroscopy,[22] the electric field was calibrated using the known ground state dipole moments. Using this method the dipole moment, μ_a of the A state of HNO was evaluated as 1.08 ± 001 D, compared to a value of 0.996 D in the ground state. Since the $^1A''$ state is perturbed and predissociated, the OODR method is being used to characterize the perturbations and hence elucidate the mechanism of the effects.

C. Effects of Collisional Energy Transfer.—Much of the work on collisional energy transfer has stemmed from the pioneering work of Oka,[78] who pointed out that many collisional processes between dipolar molecules obey electric dipole selection rules, *i.e.* that the molecule after a collision possesses a 'memory' of its state before the collision. In the early work there was little evidence for velocity selection effects, since the majority of the experiments were carried out in the microwave region where the broadening processes are largely homogeneous.[78] However, in a set of infrared experiments using two photon pumping and probing Oka and his colleagues showed that many dipolar collisions are 'soft'.[79] This means that, although the molecules change their rotational quantum state following electric dipole selection rules, the velocity component in the direction of the laser field is unchanged. Following this difficult experiment it was realised that these effects could be seen 'routinely' in laser Stark Lamb dip, and in OODR experiments as 'four-level resonances'.

[74] D. E. Freeman and W. Klemperer, *J. Chem. Phys.*, 1966, **45**, 52.
[75] N. J. Bridge, D. A. Haner, and D. A. Dows, *J. Chem. Phys.*, 1968, **48**, 4196.
[76] A. D. Buckingham, D. A. Ramsay, and J. Tyrrell, *Can. J. Phys.*, 1970, **48**, 1242.
[77] R. N. Dixon and M. Noble, *Chem. Phys.*, 1980, **50**, 331.
[78] T. Oka, *Adv. At. Mol. Phys.*, 1973, **9**, 127.
[79] S. M. Freund, J. W. C. Johns, A. R. W. McKellar, and T. Oka, *J. Chem. Phys.*, 1973, **59**, 3445.

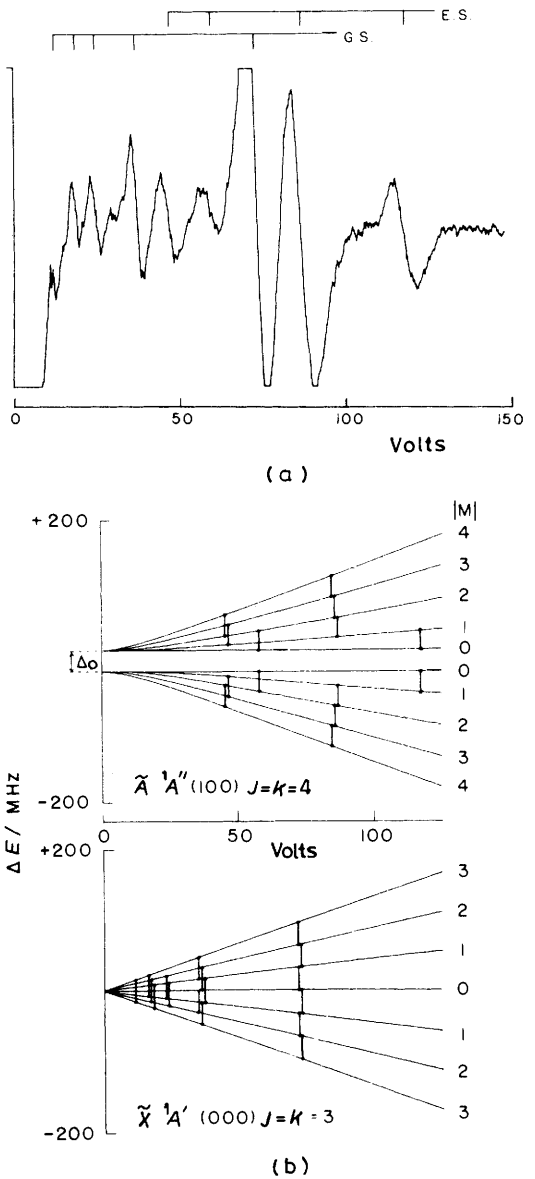

Figure 14 *M_J resolved OODR spectra of* HNO *using laser induced fluorescence, with the difference frequency generated using an amplitude modulated acousto-optic modulator. (a) Mixed polarization spectrum of the* $R_{R_3}(3)$ *line of the* A^1A'' (100)—$X\ ^1A'$ (000) *band with* $\Omega_{AM} = 15$ MHz, *and a* 3 mm *spacing between the Stark electrodes. ES, excited state resonances and GS, ground state resonances. (b) Energy level diagram showing the Stark splitting and resonant intervals corresponding to the spectrum in (a)*
(Reproduced by permission from *Chem. Phys.*, 1980, **50**, 311)

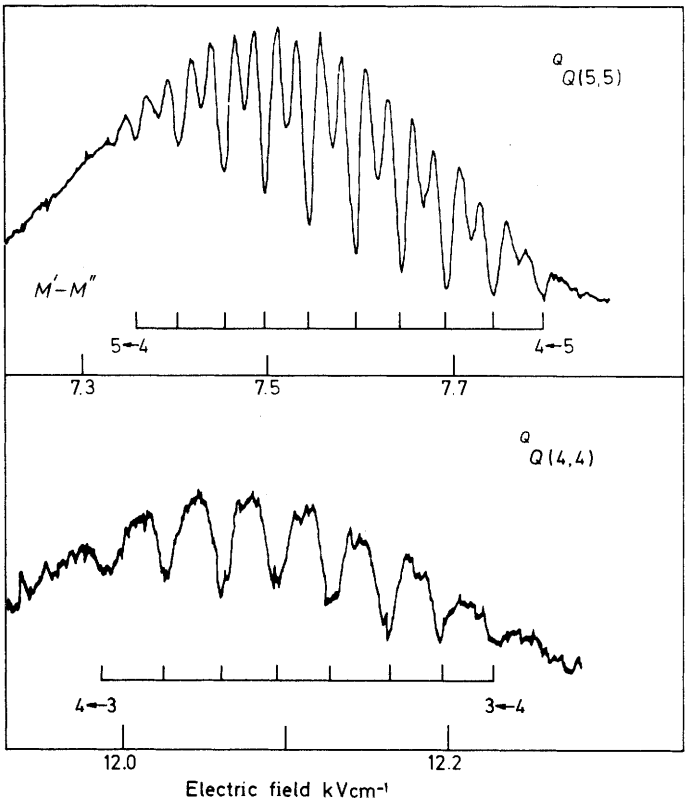

Figure 15 *Lamb dip spectra of the* QQ(5,5) *and the* QQ(4,4) *transitions of the* v_3 *band of* H_2CS *using second derivative presentation. The four-level collisionally transferred resonances seen between Lamb dips of the* QQ(5,5) *transition are approximately* 50% *of the intensity of the Lamb dips. The time constant for detection was* 300 ms *and the sample pressure about* 5 m torr (Reproduced by permission from *J. Mol. Spectrosc.*, 1980, **84**, 531)

Methyl fluoride was the first molecule in which four-level collisionally transferred resonances were clearly identified,[7,8] although subsequently they have been recognized in many systems. The example of these signals in H_2CS, Figure 15, shows that they may approach at least 50% of the intensity of a three-level resonance. This demonstrates that in molecules in which the dipole moment is directed entirely along the principal near symmetric rotor axis, *a* or *c*, the $\Delta M = \pm 1$ angular momentum tipping collisions are extremely selective. However, in molecules such as CH_3OH and CH_2NH[80,81] where there is also a *b* component of the dipole moment, the four-level resonances are much less pronounced, indicating that collisional coupling to other rotational levels is now much more probable. In some of the transitions seen in H_2CO changes of $\Delta M = 4$ or 6 have been observed.[8]

[80] D. J. Bedwell, G. Duxbury, H. Herman, and C. A. Orengo, *Infrared Physics*, 1978, **18**, 453.
[81] G. Duxbury, H. Kato, and M. L. Le Lerre, *Faraday Discuss. Chem. Soc.*, 1981, **71**, 97.

D. Level Crossing and Anti-crossing Spectroscopy.—CD_3I provides nice examples of Stark-tuned level crossings and of anti-crossings of M_F levels associated with the quadrupole hyperfine structure.[11,23,82] The level crossing signals observed in the $^2\Pi_{1/2}$ state of NO are associated with magnetic hyperfine structure,[83] and POF_3 exhibits an extensive range of anti-crossing signals, which are due to weak avoided crossings between levels that differ in k by ± 3.[84]

In these experiments the information obtained is the ratio of the electric dipole moment to a hyperfine, rotational, or quadrupole splitting, or of the magnetic moment to the hyperfine constants. Experiments such as OODR are necessary to fix one or other of the variables so that absolute values of parameters can be obtained from these measurements.

5 Studies of Semi-stable Molecules

One of the principal advantages of laser spectrometers is their sensitivity for the detection of small quantities of short-lived species. The sensitivity of laser Stark spectrometers has been discussed by Freund *et al.*,[24] and by Johns and McKellar.[65] They estimate that in the intracavity spectrometer at pressures of 4 m torr in a 20 cm absorption cell, only about 10^6 molecules are responsible for the Lamb dips seen on a particular vibration–rotation transition. This is close to Shimoda's estimate of the limiting sensitivity of a laser spectrometer.[85] This sensitivity has been exploited in the study of small 'semi-stable' molecules which, in Kroto's recent definition,[86] have lifetimes of the order of seconds under the conditions of the gas phase experiments. For example, the laser Stark spectroscopy method is suitable for studying molecules such as HNO,[22] CH_2NH,[81,87] and H_2CS,[88] but not most free radicals since the metal surfaces of the Stark plates catalyse the decomposition of the unstable molecules. The shortest-lived species studied in this type of cell is HCO,[89] which has been shown to be on the limit of the detectivity of this type of spectrometer.

Possibly the most interesting of the semi-stable molecules to be studied by laser methods is thioformaldehyde, H_2CS. Until quite recently thioformaldehyde was known only as a trimer, the first evidence for the existence of the monomer being in mass spectrometric studies. Interest in the species developed following the observation of the microwave spectrum of H_2CS in 1970,[90] followed by its subsequent detection in the interstellar dust clouds.[91] The first high resolution infrared spectrum of the 3 μm bands was obtained in 1971,[92] and required a high gas

[82] J. Sakai and M. Katayama, *Chem. Phys. Lett.*, 1975, **35**, 3.
[83] A. R. Hoy, J. W. C. Johns, and A. R. W. McKellar, *Can. J. Phys.*, 1975, **53**, 2029.
[84] T. Amano and R. H. Schwendeman, *J. Mol. Spectrosc.*, 1979, **78**, 437.
[85] K. Shimoda, *Appl. Phys.*, 1973, **1**, 77.
[86] H. W. Kroto, *Chem. Soc. Rev.*, 1982, **11**, 435.
[87] M. Allegrini, J. W. C. Johns, and A. R. W. McKellar, *J. Chem. Phys.*, 1979, **70**, 2829.
[88] D. J. Bedwell and G. Duxbury, *J. Mol. Spectrosc.*, 1980, **84**, 53.
[89] B. M. Landsberg, A. J. Merer, and T. Oka, *J. Mol. Spectrosc.*, 1977, **67**, 459.
[90] D. R. Johnson and F. X. Powell, *Science*, 1970, **169**, 679.
[91] M. W. Sinclair, N. Fourikis, J. C. Ribes, B. J. Robinson, R. D. Brown, and P. D. Godfrey, *Aust. J. Phys.*, 1973, **26**, 85.
[92] J. W. C. Johns and W. B. Olsen, *J. Mol. Spectrosc.*, 1971, **39**, 47.

pressure and a long path length, and was with a diffraction grating instrument a 'tour de force'. Similar difficulties were encountered in the recording of the $\tilde{A}^1A_2$—$\tilde{X}^1A_1$ visible absorption in 1975, when path lengths of *ca.* 100 m were required.[93]

Laser techniques were first employed in the infrared region when the 10 μm band system was observed using a laser Stark spectrometer.[88,94] The thioformaldehyde was produced by the pyrolysis of dimethyl disulphide.[88] The pyrolysis products, which include CH_4 and CH_3SH, flowed continuously through a multiple-pass Stark cell. A very high signal-to-noise ratio was obtained (Figure 15) with short time constants of 100 to 300 m s in the detection system, even though the total gas pressure in the cell was only 10 m torr.

In the 10 μm region three fundamental vibration–rotation bands were observed, ν_3, ν_4, and ν_6, rather than the two ν_3 and ν_4 expected from the matrix isolation spectroscopic results.[95] Two of the bands, ν_4 and ν_6, are nearly degenerate and hence their energy level pattern resembles that of a degenerate state of a symmetric rotor. Owing to the high resolution and sensitivity of the Lamb dip method in a crossover multiple-pass cell, the vibrational charge in dipole moment could be measured very accurately, and strong signals due to collisional energy transfer observed, as shown in Figure 15. Stark spectroscopy, therefore, played a useful role in sorting out the vibrational analysis of the infrared spectrum of H_2CS,[23] the details of which were subsequently confirmed by Fourier Transform Spectroscopy.[96] Results from OODR experiments have been combined with laser Stark[88] and molecular beam data[97] to give a very detailed picture of the vibrational dependence of the dipole moment in the ground electronic state. The observed variation of μ is compared in Table 2 with that observed in formaldehyde.

Subsequent laser experiments have been aimed at obtaining a better understanding of the structure of the electronically excited states. Initial experiments were carried out using opto-acoustic detection,[44] but most recent ones have used laser induced fluorescence.[98-100] The one exception to this was the determination of the dipole moment change with electronic excitation in the $4^1{}_0$ band of the $\tilde{A}$—$\tilde{X}$ system which was carried out using absorption spectroscopy.[101]

Studies of the fluorescence excited by pumping a single rotational level of a given vibronic state have allowed the final ground state fundamental vibrational frequency, ν_2'', to be determined.[98] They have also shown that the collisions between electronically excited species and other molecules produce very efficient self-quenching, so that fluorescence is only observed from molecules that have not

[93] R. H. Judge and G. W. King, *Can. J. Phys.*, 1975, **53**, 1927.
[94] D. J. Bedwell and G. Duxbury, *XXI^e Colloque International d'Astrophysique.*, 1977, p. 434.
[95] M. E. Jacox and D. E. Milligan, *J. Mol., Spectrosc.*, 1975, **58**, 142.
[96] P. H. Turner, L. Halonen, and I. M. Mills, *J. Mol. Spectrosc.*, 1981, **88**, 402.
[97] B. Fabricant, D. Krieger, and J. S. Muenter, *J. Chem. Phys.*, 1977, **67**, 1576.
[98] D. J. Clouthier, C. M. L. Kerr, and D. A. Ramsay, *Chem. Phys.*, 1981, **56**, 73.
[99] D. J. Clouthier and C. M. L. Kerr, *Chem. Phys.*, 1982, **70**, 55.
[100] T. Suzuki, S. Saito, and E. Hirota, *J. Chem. Phys.*, 1983, **79**, 1641.
[101] R. N. Dixon and C. R. Webster, *J. Mol. Spectrosc.*, 1978, **70**, 314.

undergone collisions since being excited. This contrasts with the behaviour observed when the gas phase phosphorescence of the $\tilde{a}^3A_2$—$\tilde{X}^1A_1$ is excited.[99] In triplet state excitation, vibrational relaxation was found to play a very important role. The frequencies of several vibrational fundamentals of the triplet state were also measured in this work. Some of the singlet–triplet perturbations have also been characterized in a recent 'non-laser' experiment that measured the magnetic rotation spectrum of the $\tilde{A}^1A_2$—$\tilde{X}^1A_1$ system.[102] Finally the laser excitation and microwave-optical double resonance, (MODR), spectra of the $3^1{}_0$ of the $\tilde{a}$—$\tilde{X}$ system have been obtained.[100] The analysis of these data has given precise values of the rotational constants, centrifugal distortion constants, the spin–spin and spin–rotation interaction constants and for the band origin. It has also allowed the difference frequency, $v_3' - v_6'$, to be measured. As a result of this recent activity the vibrational and rotational constants of the triplet, $\tilde{a}$, state are almost as well characterized as for the $\tilde{A}$ and $\tilde{X}$ states.

Since *ab initio* calculations of the vibration frequencies of H_2CS in the ground and excited electronic states have been made,[103,104] it provides one of the best examples of molecules containing second-row atoms, for which a detailed comparison of experimental and theoretical data can be made as shown in Table 3. In fact thioformaldehyde can now join its prototype, formaldehyde, as one of the best characterized tetra-atomic molecules. It is not a coincidence that many of the bands in the electronic spectrum fall within the range of the most commonly used dye in dye lasers, Rhodamine 6G!

6 Spectroscopic Studies of Free Radicals and Molecular Ions

The development of laser-based methods for the study of free radical spectra has paralleled that for stable and semi-stable molecules. The first methods to be developed were of the fixed frequency type, in particular, laser magnetic resonance (LMR), the laser analogue of gas-phase electron paramagnetic resonance spectroscopy. Following the development of tunable visible and infrared lasers, many free radicals have been studied *via* their electronic and vibration–rotation spectra. In this section we will consider the applications of the experimental techniques in approximately the historical order of their widespread use. In view of several recent reviews of this field[105–108] we will concentrate on some of the most recent experiments on chemically interesting free radicals such as CH_2, NH_2, CH_3, and HCO, and of ions such as $H_3{}^+$ and $PH_2{}^+$.

A. Laser Magnetic Resonance Spectroscopy (LMR).—In a series of recent papers the far-infrared (FIR)[109] and the mid-IR[110] LMR spectra of the $\tilde{X}^3B_1$ state of

[102] D. J. Clouthier, D. C. Moule, D. A. Ramsay, and F. W. Birss, *Can. J. Phys.*, 1982, **60**, 1212.
[103] R. Jaquet, W. Kutzelnigg, and V. Staemmler, *Theor. Chem. Acta.*, 1980, **54**, 205.
[104] J. D. Goddard and D. J. Clouthier, *J. Chem. Phys.*, 1982, **76**, 5039.
[105] K. M. Evenson, *Ref.* 83, p. 7.
[106] A. R. W. McKellar, *Ref.* 83, p. 63.
[107] E. Hirota, 'Chemical and Biological Applications of Lasers', ed. C. B. Moore, 1980, V, 39.
[108] E. Hirota, *J. Phys. Chem.*, 1983, **87**, 3375.

Table 3 *Comparison of observed and calculated vibrational fundamentals of thioformaldehyde with those of formaldehyde, and with those in the* $\tilde{A}\ ^1A_2$ *and* $\tilde{a}\ ^3A_2$ *states of thioformaldehyde*

			Frequency/cm^{-1}		
Vibration	*Description*	H_2CO[a]	$H_2CS,\tilde{X},^1A_1$	$H_2CS,\tilde{A},^1A_2$	$H_2CS,\tilde{a},^3A_2$
$\nu_1\ A_1$	Symmetric C—H stretch	[a] 2782	2971	3034	—
		[b] 2782	3057	—	—
		[c]	2937	—	2962
$\nu_2\ A_1$	Symmetric H—C—H bend	[a] 1500	1439	1310	1320
		[b] 1503	1440	—	—
		[c]	1464	—	1346
$\nu_3\ A_1$	C—S (C—O) stretch	[a] 1746	1059	820	861.6
		[b] 1709	1058	—	—
		[c]	1053	—	792
$\nu_4\ B_1$	Out-of-plane bend	[a] 1167	990	371	356
		[b] 1161	1065	—	—
		[c]	1029	—	383
$\nu_5\ B_2$	Anti-symmetric	[a] 2843	3025	3081	—
	C—H stretch	[b] 2884	3054	—	—
		[c]	3023	—	3078
$\nu_6\ B_2$	H—C—H wag	[a] 1249	991	799	762.3
		[b] 1245	989	—	—
		[c]	968	—	761

[a] Experimental—H_2CO—ref. *b*
H_2CS D. J. Bedwell and G. Duxbury, *J. Mol. Spectrosc.*, 1980, **84**, 53. W. B. Olsen and J. W. C. Johns, *J. Mol. Spectrosc.*, 1971, **39**, 47. D. J. Clouthier, C. M. L. Kerr, and D. A. Ramsey, *Chem. Phys.*, 1981, **56**, 73. R. H. Judge and G. W. King, *J. Mol. Spectrosc.*, 1979, **74**, 175.
[b] Theoretical frequencies
from R. Jaquet, W. Kutzelnigg, and V. Staemmler, *Theor. Chem. Acta.*, 1980, **54**, 205. Harmonic frequencies reduced by 5.15% to give correct weighting for H_2CO, for justification for scaling see ref. *c*.
[c] Theoretical frequencies
from J. D. Goddard and D. J. Clouthier, *J. Chem. Phys.*, 1982, **76**, 5039. 10.5% scaling of calculated harmonic frequencies applied.

CH_2 have been obtained, and combined with a large amplitude vibrational model of the ground state.[111] Previous data on the triplet state were derived from the analysis of the pre-dissociated electronic spectrum,[112] and from the e.s.r. spectrum of matrix isolated CH_2.[113]

From the pure rotation LMR spectrum in the FIR laser region,[109] accurate ground-state rotational constants have been obtained, as well as spin–spin, spin–rotation, and hyperfine constants. As an example of the sensitivity and resolution attainable on the FIR and mid-IR regions, Doppler and sub-Doppler spectra produced using both methods are presented in Figure 16. Note that triplet patterns can be seen without the benefit of saturation spectroscopy in the FIR region because of the much smaller Doppler width of the lines. The mid-infrared data on $^{12}CH_2$ and $^{13}CH_2$[110] has shown that the bending vibration ν_2, has a much

[109] T. J. Sears, P. R. Bunker, A. R. W. McKellar, K. M. Evenson, D. A. Jennings, and J. M. Brown, *J. Chem. Phys.*, 1982, **77**, 5348.
[110] T. J. Sears, P. R. Bunker, and A. R. W. McKellar, *J. Chem. Phys.*, 1982, **77**, 5363. A. R. W. McKellar and T. J. Sears, *Can. J. Phys.*, 1983, **61**, 480.

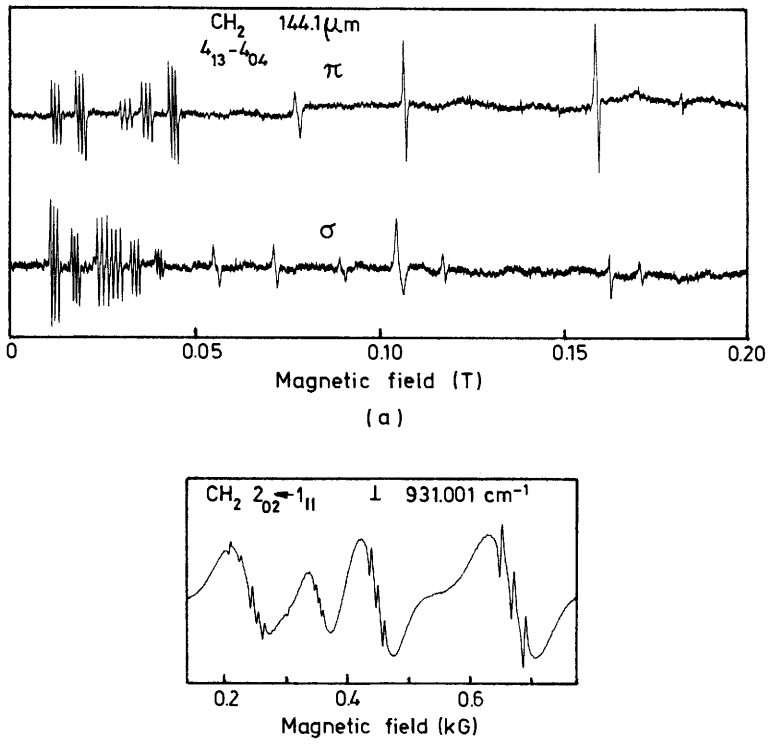

Figure 16 *LMR spectra of* CH_2, *using FIR and mid-IR lasers, showing triplet hyperfine structure. (a) Spectra obtained using the* 144.1 μm (69.38765 cm^{-1}) *laser line of* CD_3OH *in* π *and* σ *polarizations. The resonances observed are for various Zeeman components of the* $4_{13}-4_{04}$ *rotational transition. (b) Spectrum observed with the* $^{12}C^{16}O_2$ *P*(34) *laser line at* 931.001 cm^{-1} *due to the* $2_{02}-1_{11}$ *transition. The triplet structure is revealed as a result of the enhanced resolution of saturation spectroscopy (Lamb dips)*
(Reproduced by permission from *J. Chem. Phys.*, 1982, **77**, 5348 and 5363)

lower frequency than was previously assumed in modelling the negative ion photodetachment spectrum of CH_2^-, casting doubt on the details of the interpretation proposed for the vibronic structure.[110,114]

The non-rigid bender Hamiltonian[111] has enabled the equilibrium geometry of the $\tilde{X}^3B_1$ state to be determined, and a height of the potential barrier to linearity for the v_2 vibrational state to be derived. These are compared in Table 4 with analogous parameters recently derived for the $\tilde{a}^1A_1$ and the $\tilde{b}^1B_1$ states of CH_2.

The singlet–triplet separation in CH_2 has been a source of controversy for some

[111] P. Jensen, P. R. Bunker, and A. R. Hoy, *J. Chem. Phys.*, 1982, **77**, 5370.
[112] G. Herzberg, *Proc. R. Soc., London, Ser. A*, 1961, **262**, 291.
[113] R. A. Bernheim, H. W. Bernard, P. S. Wang, L. S. Wood, and P. S. Skell, *J. Chem. Phys.*, 1970, **53**, 1280.

Table 4 *Geometrical parameters of the electronic states of* CH_2

	$\tilde{X}^3B_1$		$\tilde{a}^1A_1$ [c,d]	$\tilde{b}^1B$ [c,d]
Barrier height/cm^{-1}	1877.6	[a]	9451	1193
	2032	[b]		
Equilibrium bond angle/°	133.88	[a]	101.7	141
	133.4	[b]		
Equilibrium bond length/Å	1.075	[a]	1.114	1.083
	1.085	[b]		

[a] Non-rigid bender—P. Jensen, P. R. Bunker, and A. R. Hoy, *J. Chem. Phys.*, 1982, **77**, 5370. [b] Semi-rigid bender—T. J. Sears, P. R. Bunker, and A. R. W. McKellar, *J. Chem. Phys.*, 1982, **77**, 5363. [c] Semi-rigid bender and Renner–Teller coupling—G. Duxbury, *J. Chem. Soc., Faraday Trans.* 2, 1982, **78**, 1433. [d] Singlet–triplet splitting $\tilde{a} - \tilde{X} = 2994 \pm 30\ cm^{-1}$, single–singlet splitting $\tilde{b} - \tilde{a} = 8258 \pm 100\ cm^{-1}$—A. R. W. McKellar, P. R. Bunker, T. J. Sears, K. M. Evenson, R. J. Saykally, and S. R. Langhoff, *J. Chem. Phys.*, 1983, in the press.

time, and even more so recently since the value deduced in[114] of *ca.* 0.85 eV is approximately twice the currently accepted value from other measurements and calculations. Perturbation allowed transitions, which are due to the interaction between excited vibrational levels of the triplet state and the ground vibrational state of the lowest electronic singlet, $\tilde{a}^1A_1$ state, have been observed in the FIR LMR spectra of the $\tilde{a}$ state of CH_2.[115] The detailed analysis of these transitions has shown that the singlet–triplet splitting derived from the photodetachment spectra is far too large, and has given the first *unambiguous* and accurate value for the singlet–triplet splitting. This is found to be $3165 \pm 20\ cm^{-1}$ for the zero-point energy difference, and $2994 \pm 30\ cm^{-1}$ for the separation between the minima of the potential wells.[115] This has led to a reappraisal of the analysis of the CH_2^- spectra from which it has been concluded that the effective temperature of the negative ions is far higher than had been assumed in modelling the envelope of the photodetatchment spectrum.

An interesting observation in the high field LMR spectra of some free radicals has been the presence of strong resonant signals whose positions do not vary in field strength when the laser frequency is detuned. These signals have subsequently been identified as anti-crossing signals and have been observed in the spectra of several radicals including ClO_2[12] and DO_2[116].

B. Tunable Infrared Laser Spectroscopy of Free Radicals and Ions.—In many of the free radical experiments recently reported the radicals have either been generated by atom reactions or by DC or RF discharges within the absorption cells. Since the method does not depend upon Stark or Zeeman tuning for anything other than

[114] P. C. Engelking, R. C. Corderman, J. J. Wendolski, G. B. Ellison, S. V. O'Neil, and W. C. Lineberger, *J. Chem. Phys.*, 1981, **74**, 5460.
[115] A. R. W. McKellar, P. R. Bunker, T. J. Sears, K. M. Evenson, R. J. Saykally, and S. R. Langhoff, *J. Chem. Phys.*, 1983, in the press. T. J. Sears and P. R. Bunker, *J. Chem. Phys.*, 1983, in the press.
[116] H. Uehara, *J. Chem. Phys.*, 1982, **77**, 3314.

modulation, metal-free cells can be used to prevent radical recombination, and pressures of *ca.* 1 torr can be used as there is no risk of electrical breakdown. For paramagnetic species such as BO_2 two methods of detection have been used, Zeeman modulation and source modulation. Zeeman modulation is accomplished by winding a Zeeman coil around the glass pipe of the absorption cell. With Zeeman modulation only paramagnetic species are detected and low J lines are preferentially enhanced, since the modulation efficiency is inversely proportional to J. With source modulation, on the other hand, all species are detected. In systems where there is no ambiguity in assignment source modulation allows much higher J lines to be detected. As an example of this, spectra of BO_2[117] using both types of modulation are shown in Figure 17. In addition to BO_2, which is very difficult to detect in the microwave region since it has no permanent electric dipole moment, several other interesting free radicals and ions have been detected using diode, F-centre, or difference frequency spectrometers. The first ion to be detected in this way was H_3^+ by Oka.[118] The spectrum of this ion was finally identified after a long search in a high-current low-temperature discharge in hydrogen. The geometry and other molecular parameters of H_3^+ are close to those predicted by *ab initio* calculation and serve as a severe test of theoretical methods. One electronic spectrum which happens to occur in the infrared region, that of the $^2\Sigma^- — ^2\Pi$ transition of C_2H, was detected at 3772 cm^{-1} using an F centre laser.[119] It is possible that transitions between other close lying electronic states of polyatomic molecules will be detected using tunable infrared lasers.

One molecule of particular interest that has been studied recently is CH_3. Spectra have been obtained of transitions involving the bending vibration, ν_2, using diode lasers,[120,121] and of the ν_3 region using a difference frequency spectrometer.[122] The study of the ν_2 vibrational ladder has shown conclusively that the equilibrium geometry of the CH_3 radical is planar in the gas phase and has allowed a potential function for the bending well to be developed. The ν_3 study has characterized the asymmetric stretching vibrational band, and together with the ν_2 data, yields a good approximation to the equilibrium structure of the radical. The ν_3 region lies in an atmospheric window, and hence these transitions may be useful for searching for lines of interstellar CH_3. The most recent measurements on CH_3 are of the transition dipole moment of the ν_2 band.[123] This transition moment is very large, 0.28 D, and comparable to that in NH_3. Knowledge of this quantity has allowed reaction kinetics of the CH_3 radical to be carried out in the gas phase.[124]

[117] K. Kawaguchi, E. Hirota, and C. Yamada, *Mol. Phys.*, 1981, **44**, 509.
[118] T. Oka, *Phys. Rev. Lett.*, 1980, **45**, 531.
[119] P. G. Carrick, J. Pfeffer, R. F. Curl, E. Koestre, F. K. Tittel, and J. V. V. Kasper, *J. Chem. Phys.*, 1982, **76**, 3336.
[120] C. Yamada, E. Hirota, and K. Kawaguchi, *J. Chem. Phys.*, 1981, **75**, 5256.
[121] E. Hirota and C. Yamada, *J. Mol. Spectrosc.*, 1982, **96**, 175.
[122] T. Amano, P. F. Bernath, C. Yamada, Y. Endo, and E. Hirota, *J. Chem. Phys*, 1982, **77**, 5284.
[123] C. Yamada and E. Hirota, *J. Chem. Phys.*, 1983, **78**, 669.
[124] G. A. Laguna and S. L. Baughcum, *Chem. Phys. Lett.*, 1982, **88**, 568.

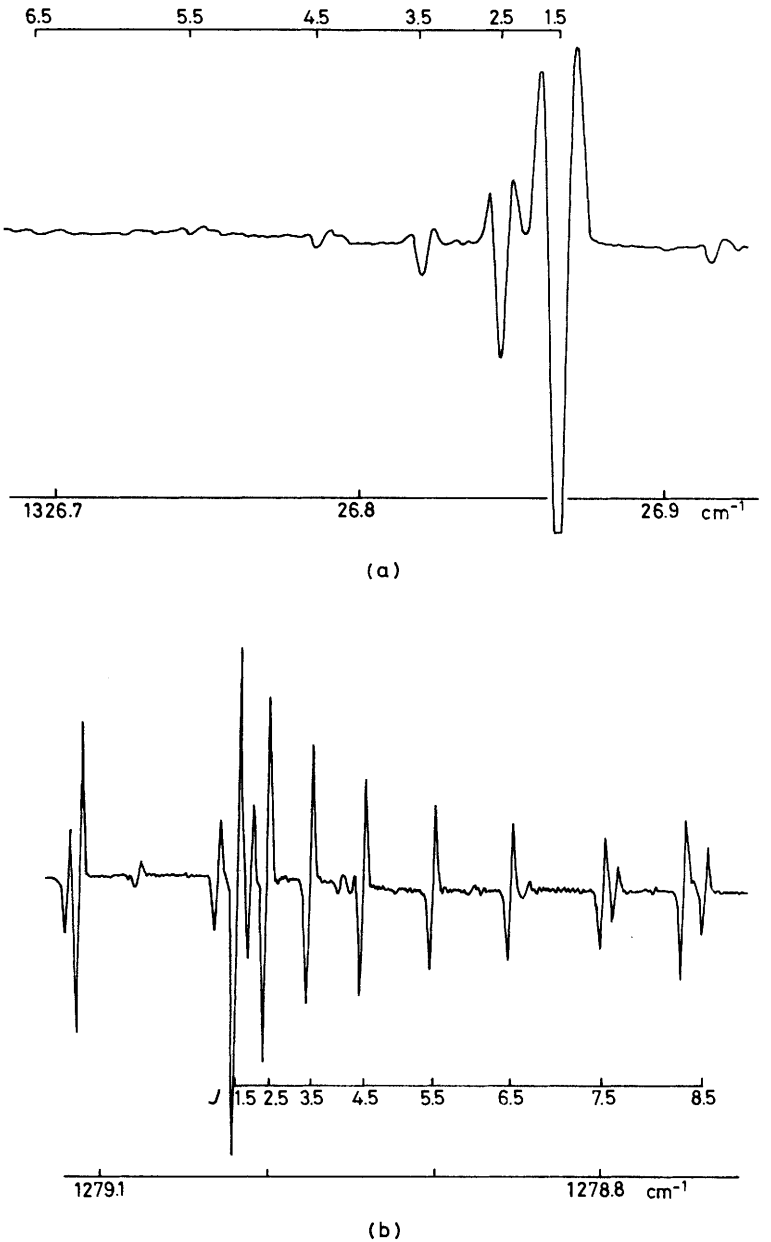

Figure 17 *(a) Q-branch transitions of the ν_3 band of $^{10}BO_2$ in the $^2\Pi_{\frac{1}{2}}$ state, obtained by Zeeman modulation. (b) Analogous transitions in $^{11}BO_2$ obtained by frequency modulation of the diode*
(Reproduced by permission from *Mol. Phys.*, 1981, **44**, 509)

This method has greater potential than the previous gas phase method for detecting methyl which relies on measurement of the vacuum ultraviolet absorption spectrum,[125] particularly since this spectrum is partly predissociated.

C. Velocity Modulated Spectra of Ions.—In a DC glow discharge the ions possess a net drift velocity, v_d, as a result of their mobility in the axial electric field of the discharge. The Doppler shift, $\Delta\nu$, is then related to the drift velocity by:

$$\Delta\nu/\nu = v_d/c$$

where c is the velocity of light. For typical discharge conditions $\Delta\nu$ can be *ca.* 90 MHz at $\nu = 2500\,\text{cm}^{-1}$, *i.e.* comparable to the Doppler broadened linewidth. The resultant Doppler shift can be positive or negative, depending on whether v_d is in the same or the opposite sense as the laser beam direction. This Doppler shift has been used in two ways, as a means of differentiating the spectra of ions from those of neutral species present in the discharge, and as a way of studying ion transport processes in detail.

Selective detection of ion spectra has been obtained by modulating the drift velocity of ions using an AC discharge.[126] When the polarity of a glow discharge is reversed at several kilohertz the ion absorption frequencies are alternatively red- and blue-shifted at this rate. Detecting at the field modulation frequency then yields the infrared spectrum of the ionic species. This method has been used with an F-centre laser to detect R-branch absorption transitions of the ν_1 vibration–rotation band of HCO^+, and has given a very good signal to noise ratio.

In the second type of experiment[127] a frequency modulated diode laser beam was split into two parts, which were then sent in opposite directions through a discharge in a mixture of He, Ar, and H_2. This allowed the Doppler shifts of absorption lines of ArH^+, formed in the discharge, to be measured as a function of the pressure and composition of the discharge. Preliminary results obtained suggest a dependence of the ion mobility on vibrational excitation, with $v = 1$ ions being more mobile than those with $v = 0$. This is one of the first demonstrable effects of quantum processes in ion transport.

D. Optogalvanic Spectroscopy.—The mechanism of the optogalvanic effect is still the subject of some controversy. One proposal is that the main mechanism in the visible and u.v. regions is the difference in the collisional ionization rates of the two states. However, visible signals observed using I_2[128] are very similar to those recently recorded in the infrared, using diode lasers,[47] where the ionization mechanism is inappropriate. It is therefore proposed that an alternative scheme operates in which the main effect of the laser radiation is to pump energy into the electron gas, hence causing an increase in the kinetic energy of the species.

[125] G. Herzberg, 'Molecular Spectra and Molecular Structure Vol. III: Electronic Spectra and Structure of Polyatomic Molecules', Van Nostrand-Reinhold, New York, 1966.
[126] C. S. Gudeman, M. E. Begemann, J. Pfaff, and R. J. Saykally, *Phys. Rev. Lett.*, 1983, **50**, 727.
[127] N. Haese, F. S. Pan, and T. Oka, *Phys. Rev. Lett.*, 1983, **50**, 1575.
[128] C. T. Rettner, C. R. Webster, and R. N. Zare, *J. Phys. Chem.*, 1981, **85**, 1105.

Although in general laser powers of greater than 100 milliwatts have been used to obtain LOG signals, it has recently shown that good signals in the infrared spectra of NH_3 and NO_2 could be obtained using diode lasers with a power level of *ca.* 1 milliwatt.[47]

A recent study[129] of the predissociation of HCO exemplifies the utility of the LOG approach for studying species produced in electric discharges. The HCO $\tilde{A}^2A''$—$\tilde{X}^2A'$ spectrum is weak and predissociated. By using the optogalvanic effect in an RF discharge in the parent species, acetaldehyde, mixed with an argon–helium carrier gas, it has been possible to measure the linewidths in the $0,9^0$, 0—$0,0^1$, 0 band using a single mode dye laser with a sensitivity of 10^5 over that obtained in conventional flash photolysis experiments. The line widths show a strong dependence on the overall rotational quantum number N, increasing by a factor of 4 when N increases from 4 to 16. It was also shown that there is an N-independent contribution. By modelling the behaviour of the line width, it has been shown that the main mechanisms for the predissociation are coupling to dissociative Δ levels through K-type resonance and perturbations with Π levels through Coriolis interaction. The remaining contribution to the broadening is thought to be associated with a homogeneous, spin-orbit, coupling between the excited-state levels and high-lying levels of the ground state.

E. Ion Beam Spectroscopy.—Two recent sets of experiments that show the utility of the technique will be cited. The first set used visible lasers to investigate the electronic spectra of H_2S^+,[130] of NH^+, PH^+, and SH^+[131] and of PH_2^+[132] by monitoring the fragment ions arising from the predissociated excited electronic state. Since tunable dye lasers were used the spectra could be recorded either by sweeping the velocity of the ion beam, as described previously, or in a broad-band low-resolution scan by sweeping the dye laser frequency. In the case of H_2S^+ this has shown that the complex vibronic pattern seen in the $\tilde{A}^2A_1$—$\tilde{X}^2B_1$ emission spectrum[133] is even more complex than previously supposed, when the greatly enhanced resolution of the ion beam techniques is employed. In the spectra of NH^+, PH^+, and SH^+ some interesting examples of proton hyperfine interaction splittings were seen in both electronic states. PH_2^+ possibly possesses the most interesting spectrum of this group of ions since it is the first example of the high-resolution gas-phase spectrum of this ion. Although this ion is isoelectronic with SiH_2, the spectra obtained when monitoring the P^+ dissociation fragment bears little resemblance to the absorption spectrum of SiH_2 obtained by Dubois.[134,135] One possibility is that the ion is produced vibrationally hot, so that

[129] R. Vasudev and R. N. Zare, *J. Chem. Phys.*, 1982, **76**, 5267.
[130] C. P. Edwards, C. S. Maclean, and P. J. Sarre, *Chem. Phys. Lett.*, 1982, **87**, 11.
[131] C. P. Edwards, C. S. Maclean, and P. J. Sarre, *J. Chem. Phys.*, 1982, **76**, 3829.
[132] C. P. Edwards, P. A. Jackson, and P. J. Sarre, Paper C18 presented at the 8th Colloquium on High Resolution Molecular Spectroscopy, Tours, 1983.
[133] G. Duxbury, Ch. Jungen, and J. Rostas, *Mol. Phys*, 1983, **48**, 719.
[134] I. Dubois, *Can. J. Phys.*, 1968, **46**, 2485.
[135] I. Dubois, G. Duxbury, and R. N. Dixon, *J. Chem. Soc., Faraday Trans. 2*, 1975, **71**, 799.
[136] E. Hirota, personal communication.

sequence band structure dominates the spectrum. Another reason for the difference may lie in singlet–triplet perturbations for which there is some evidence in the $\tilde{A}^1B_1$—$\tilde{X}^1A_1$ fluorescence spectrum of SiH_2. Hirota and his colleagues[136] have noted that in the laser induced fluorescence spectrum of SiH_2 the strongest lines are absent from the absorption spectrum recorded in the same region, and it is the weaker lines that correspond to the lines seen in the absorption spectrum. The strong lines may therefore be evidence for singlet–triplet perturbations, which are known to be important in other systems such as H_2CS.[102] The spectrum obtained when detecting the PH^+ fragment must represent the transitions to a state which undergoes asymmetric dissociation. It does not resemble that obtained when using P^+ detection and probably represents a transition which does not involve the ground electronic state of the ion.

The fixed frequency method originally used in ion beam studies[30] has recently been extended. Infrared multiphoton dissociation has been used to look at some of the transitions of HD^+ near the dissociation limit. Infrared spectra of CH^+[137] and of H_3^+[138] have also been obtained near their dissociation limits by using photodissociation induced by a CO_2 laser.

In the case of CH^+,[137] where the low lying energy levels of states have previously been investigated in some detail, some progress has been made in understanding the behaviour in this region which lies within $1000\,cm^{-1}$ of the upper dissociation limit of

$$CH^+ \rightarrow C^+(^2P^3{}_2) + H$$

H_3^+[138] on the other hand is a much more complex system with a very erratic many line spectrum. Some recent progress has been made by showing that, if the resolution is deliberately degraded by bunching the lines into 'clumps', a regularity which can be associated with rotation of an H_2 unit loosely bonded to H^+ is evident.[139]

F. NH_2—A Spectroscopic Case History.—The free radical NH_2 has been the subject of extensive high resolution spectroscopic analyses, particularly by means of its $\tilde{A}^2A_1$—$\tilde{X}^2B_1$ electronic spectrum in the visible region. It is of interest on several counts: as a reactive intermediate, as a constituent of cometary spectra, and as possibly the best known and characterized example of the Renner–Teller effect, the breakdown of the Born–Oppenheimer separation in a triatomic molecule, which has been the subject of several recent theoretical papers.[140,141]

Although the original work on NH_2 used the flash photolysis method to generate the free radical,[142] more recent laser based experiments have used continuous flow systems: either atom reactions, or, more recently, DC electric discharges in NH_3. The use of lasers has enabled pure rotation spectra to be observed using

[137] A. Carrington, J. Buttenshaw, R. A. Kennedy, and T. P. Softley, *Mol. Phys.*, 1982, **45**, 747.
[138] A. Carrington, J. Buttenshaw, and R. A. Kennedy, *Mol. Phys.*, 1982, **45**, 753.
[139] R. A. Kennedy, personal communication.
[140] Ch. Jungen, K. E. J. Hallin, and A. J. Merer, *Mol. Phys.*, 1980, **40**, 25.
[141] Ch. Jungen, K. E. J. Hallin, and A. J. Merer, *Mol. Phys.*, 1980, **40**, 65.
[142] K. Dressler and D. A. Ramsay, *Philos. Trans. R. Soc. London, Ser. A.*, 1959, **251**, 553.

LMR.[143] vibration rotation spectra of the ν_2 band by LMR,[144] and infrared spectra of the ν_1 and ν_3 bands by difference laser spectroscopy.[145] These far and mid-infrared data have led to far more accurate rotational and vibrational constants for the electronic ground state than are available from electronic spectra alone. In particular ν_3 is a non-totally symmetric vibration, and hence it can be observed in the electronic spectrum only by its perturbing effect on ν_1.

As well as providing additional data on the lowest vibrational levels of the electronic ground state of NH_2, laser induced fluorescence spectra[146,147] have provided data on the high vibrational levels of the $^2B_1$ state that have aided the construction of accurate potential energy curves used in the Renner–Teller calculations.[140] When laser induced fluorescence is used in conjunction with sub-Doppler methods, a wealth of detail about the fine and hyperfine interactions in NH_2 is revealed. Most of the techniques in the sub-Doppler armoury have been employed to study the details of this extremely perturbed spectrum. The methods used included saturation spectroscopy using intermodulated fluorescence,[148] microwave–optical double resonance,[149] hyperfine level crossing,[150] optical–optical double resonance using fluorescence detection,[151] and infrared–optical double resonance.[152]

The OODR[151] experiments of NH_2 probe the 0_{00} level of the $\tilde{A}$ (090) vibronic state. Since this is the lowest possible level with $N = 0$ and has a value of $K_a = 0$, it is expected to represent an 'isolated' upper state level of NH_2, unaffected by Renner–Teller perturbations. This has enabled values of the nitrogen hyperfine coupling constant, a_n, and the ratio of the g_J value to that of the free spin, g_s, to be measured. These then provide a yardstick for comparison with the values of a_n of perturbed levels, and with the g_J values of levels with $K_a \geqslant 1$, some of which have a large admixture of orbital angular momentum.

The infrared-optical double resonance experiment[152] is a hybrid of two powerful techniques, LMR and laser induced fluorescence. The fluorescence cell is placed either within or outside the cavity of a CO_2/N_2O infrared laser, and the visible laser beam introduced into the cell through the end window of the CO_2 laser in the intracavity system. The magnetic field is used to tune the molecular energy levels into resonance with the IR laser, and the effect of saturation of the IR transition is detected by the change in fluorescence of the visible emission. In the intracavity apparatus two sets of signals are observed, one set resulting from the visible and

[143] P. B. Davies, D. K. Russell, B. A. Thrush, and H. E. Radford, *Proc. R. Soc. London, Ser A.*, 1977, **377**, 299.
[144] K. Kawaguchi, C. Yamada, E. Hirota, J. M. Brown, J. Buttenshaw, C. R. Parent, and T. J. Sears, *J. Mol. Spectrosc.*, 1979, **81**, 60.
[145] T. Amano, P. F. Bernath, and A. R. W. McKellar, *J. Mol. Spectrosc.*, 1982, **94**, 100.
[146] M. Kroll, *J. Chem. Phys.*, 1975, **63**, 319.
[147] M. Vervloet, M. F. Merienne-Lafore, and D. A. Ramsay, *Chem. Phys. Lett.*, 1978, **57**, 5.
[148] G. W. Hills, D. L. Philen, R. F. Curl, and F. K. Tittel, *Chem. Phys.*, 1976, **12**, 107.
[149] G. W. Hills, C. R. Brazier, J. M. Brown, J. M. Cook, and R. F. Curl, *J. Chem. Phys.*, 1982, **76**, 240.
[150] R. N. Dixon and D. Field, *Mol. Phys*, 1977, **34**, 1563.
[151] R. N. Dixon, *Ref.* 44, p. 1563.
[152] T. Amano, K. Kawaguchi, M. Kakimoto, S. Saito, and E. Hirota, *J. Chem. Phys.*, 1982, **77**, 159.

IR beam propagating in opposite directions, and the other set from the two beams having the same propagation direction. Interesting effects of the very different Doppler widths in the infrared and visible region manifested themselves in the very different linewidth and intensity behaviour when either the IR or the visible laser was scanned. This technique offers the chance of obtaining laser magnetic resonance data on excited electronic states and offers a route to the determination of parameters such as those governing the magnetic quenching of fluorescence.

A final use of high resolution laser induced fluorescence of NH_2 has been the determination of the electric dipole moment in the ground electronic state.[153] This has been accomplished by measuring the Stark effect in the asymmetric molecule NHD, which possesses an *a*-component of the dipole moment yielding comparably large Stark shifts. The dipole moment determined in this way is 1.82 ± 0.05 D, which is very similar to that of water. Because of the large size of μ, interstellar rotational emission lines should be strong provided that concentrations of NH_2 or NHD are not prohibitively small, and a search for such spectra is currently in progress.

7 Ultra High Resolution Spectroscopy

Spectra obtained using noble gas and CO_2 waveguide laser based spectrometers are among some of the highest resolution spectra ever obtained. In order to achieve such high resolution very large diameter cells of up to 38 cm have been used, and in order to use low pressures, cell lengths of up to 13 m are necessary. Using cells of this type wavefronts approaching those of a plane wave can be achieved. In one of the pioneering experiments by Hall, Borde, and Uehara[154] using a HeNe laser, the recoil splitting of hyperfine components in CH_4 was observed. When a molecule is excited by the absorption of a photon it absorbs the momentum of the photon as well as its energy. Because of momentum conservation, molecules interacting with a monchromatic field of a given direction have to belong to two slightly different momentum classes in the upper and lower levels. The momentum change is equal to that of the light quantum momentum:

$\pm \frac{h^2\nu^2}{2Mc^2}$ (where the sign depends on the direction of the beam with respect to the z axis)

The return beam of the saturated absorption spectrometer thus sees two velocities, frequencies of anomalously high transmission. One peak occurs in the usual way by interrogation of the population 'hole' in the absorbing lower state. The other peak corresponds to spectrally narrow amplification of the return beam by the velocity-selected and displaced molecules, placed into the excited state by interaction with the other laser beam. The resultant spectrum is shown in Figure 18.

Following the observation of these effects in the 3 μm region, ultra-stable waveguide CO_2 lasers have been constructed that have enabled similar resolution to be attained in the 10 μm region. Very high resolution spectra of the ν_3 bands of SF_6

[153] J. M. Brown, S. W. Chalkley, and F. D. Wayne, *Mol. Phys.*, 1979, **38**, 152.
[154] J. L. Hall, Ch. J. Borde, and K. Uehara, *Phys. Rev. Lett.*, 1976, **37**, 1339.

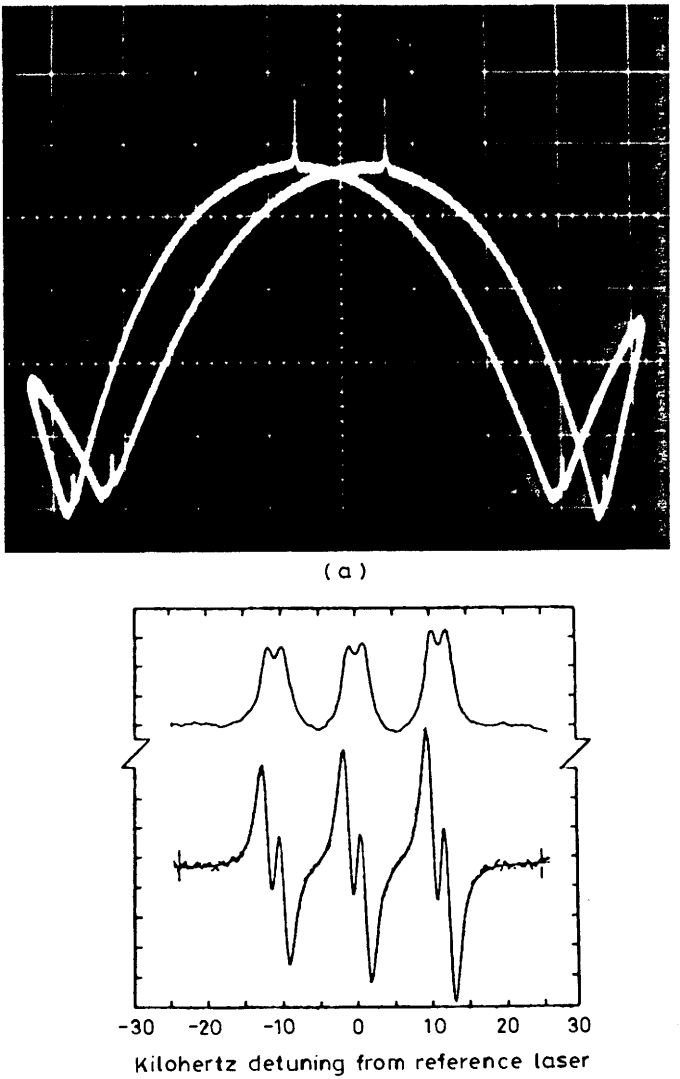

Figure 18 *(a) Saturation peak in the output of a* He–Ne *laser seen in the original intracavity 'inverted' Lamb dip experiment on* CH_4. *The laser frequency was swept twice over the gain profile. (b) Ultra-high resolution derivative spectrum of the three main hyperfine lines of* $^{12}CH_4$ *showing the recoil doubling (lower curve). Methane pressure* 70 μ torr; *room temperature; modulation of* 800 Hz *peak to peak. A least-squares fit (solid line) gives a width of* 1.27 kHz *HWHM and a recoil doublet splitting of* 2.150 kHz, *the high frequency peak* 1% *larger than the low frequency ones. The upper curve, integrated from a sample of such data, shows that each hyperfine component is spectrally doubled by the recoil effect*
(Reproduced by permission from *Phys. Rev. Lett.*, 1969, **22**, 4; 1976, **37**, 1339)

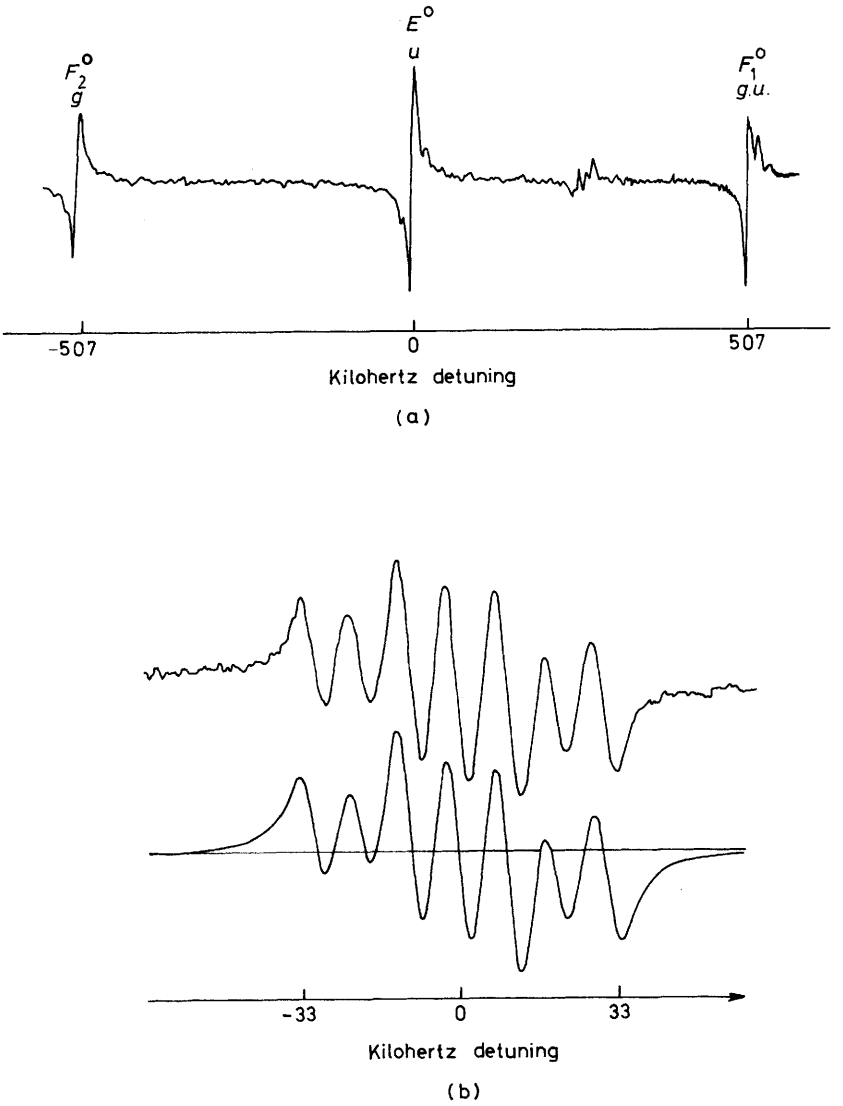

Figure 19 *(a) Ultra-high resolution spectrum of the* SF_6Q_{38} *cluster at* 28.412582452 THz *recorded using a frequency controlled saturation spectrometer based on a waveguide* CO_2 *laser. (b) Magnetic hyperfine structure of the* R_{28} A_2^0 line of $^{32}SF_6$ *at* 28.46469125 THz. *The upper trace is the observed spectrum, and the lower trace calculated using the scalar spin-rotation interaction* $W_{SRS} = -hc_aIJ$, with $c_a = -5$ kHz. *The resolution is* ca. 5 kHz.
(Reproduced by permission from 'Laser Spectroscopy IV', ed. H. Walther and K. W. Rothe, Springer Verlag, 1979, 142)

and Os_4 have been observed,[155,156] including signals due to nuclear hyperfine interactions. These result from vibrationally and rotationally produced distortions of the tetrahedral or octahedral geometry.[157] This mechanism is similar to that responsible for the generation of rotationally induced dipole moments. Examples of the spectra of SF_6 observed in this way are reproduced in Figure 19, where the half-width at half maximum of 5 kHz corresponds to a resolution of about 1 part in 10^{10}.

Progress in frequency-locking ion and dye lasers has allowed similar spectra to be obtained in the visible region.[158] Particular advances have included phase locking of lasers to stable cavities,[159] frequency-modulation spectroscopy,[160] and 'Ramsay fringe' spectroscopy.[159,161]

7 Conclusion

In this article I have endeavoured to present a picture of the impact of lasers on high resolution gas phase molecular spectroscopy by concentrating on what I regard as certain key areas. This approach, by its very nature, must lead to several topics being either omitted, or treated in a perfunctory fashion. In depth treatment of much of the subject matter has been given in the books of Hollas[162] and Demtroder,[2] and in the excellent review articles of Macpherson and Barrow.[163,164] In these reviews an almost complete bibliography of experimental work in gas phase molecular spectroscopy from 1978 up to the beginning of 1982 has been given.

Acknowledgements. It is a pleasure to acknowledge the debt I owe to Richard Dixon and Takeshi Oka for stimulating my interest in this field. I would particularly like to acknowledge my collaborators Gareth Jones, Joelle Rostas, Marcel Horani, Christian Jungen, Sam Freund, John Johns, Gordon Caldow, Mike Ashfold, Henryk Herman, David Bedwell, Michel Le Lerre, Hiroshi Kato, Jan Petersen, June McCombie, and David Devoy, without whose enthusiasm and drive little would have been accomplished.

[155] Ch. J. Borde, M. Ouhayoun, A. Van Lerberghe, C. Salomon, G. Avillier, C. D. Cantrell, and J. Borde, in *'Laser Spectroscopy IV'*, ed. H. Walther and K. H. Rothe, Springer Verlag, 1979, p. 142.
[156] J. Borde, Ch. J. Borde, C. Salomon, A. Van Lerberghe, M. Ouhayoun, and C. D. Cantrell, *Phys. Rev. Lett.*, 1980, **45**, 14.
[157] J. T. Hougen and T. Oka, *J. Chem. Phys.*, 1981, **74**, 1830.
[158] J. Helmcke, S. A. Lee, and J. L. Hall, *Applied Optics*, 1982, **21**, 1686.
[159] J. L. Hall, L. Hollberg, M. Long-sheng, T. Baer, and H. G. Robinson, *J. de Phys.*, 1981, **12**, c8.
[160] J. L. Hall, L. Hollberg, T. Baer, and H. G. Robinson, *Appl. Phys. Lett.*, 1981, **39**, 680.
[161] S. A. Lee, J. Helmcke, and J. L. Hall, *Ref.* 155, p. 130.
[162] J. M. Hollas, 'High Resolution Molecular Spectroscopy', Butterworths, London, 1982.
[163] M. T. Macpherson and R. F. Barrow, *Annu. Rep. Prog. Chem., Sect. C*, 1979, **76**, 51.
[164] M. T. Macpherson and R. F. Barrow, *Annu. Rep. Prog. Chem., Sect. C*, 1981, **78**, 221.